NAIST

Doctoral dissertation
No. : 0381202

Structural characterization of human Rad GTPase of the RGK-family

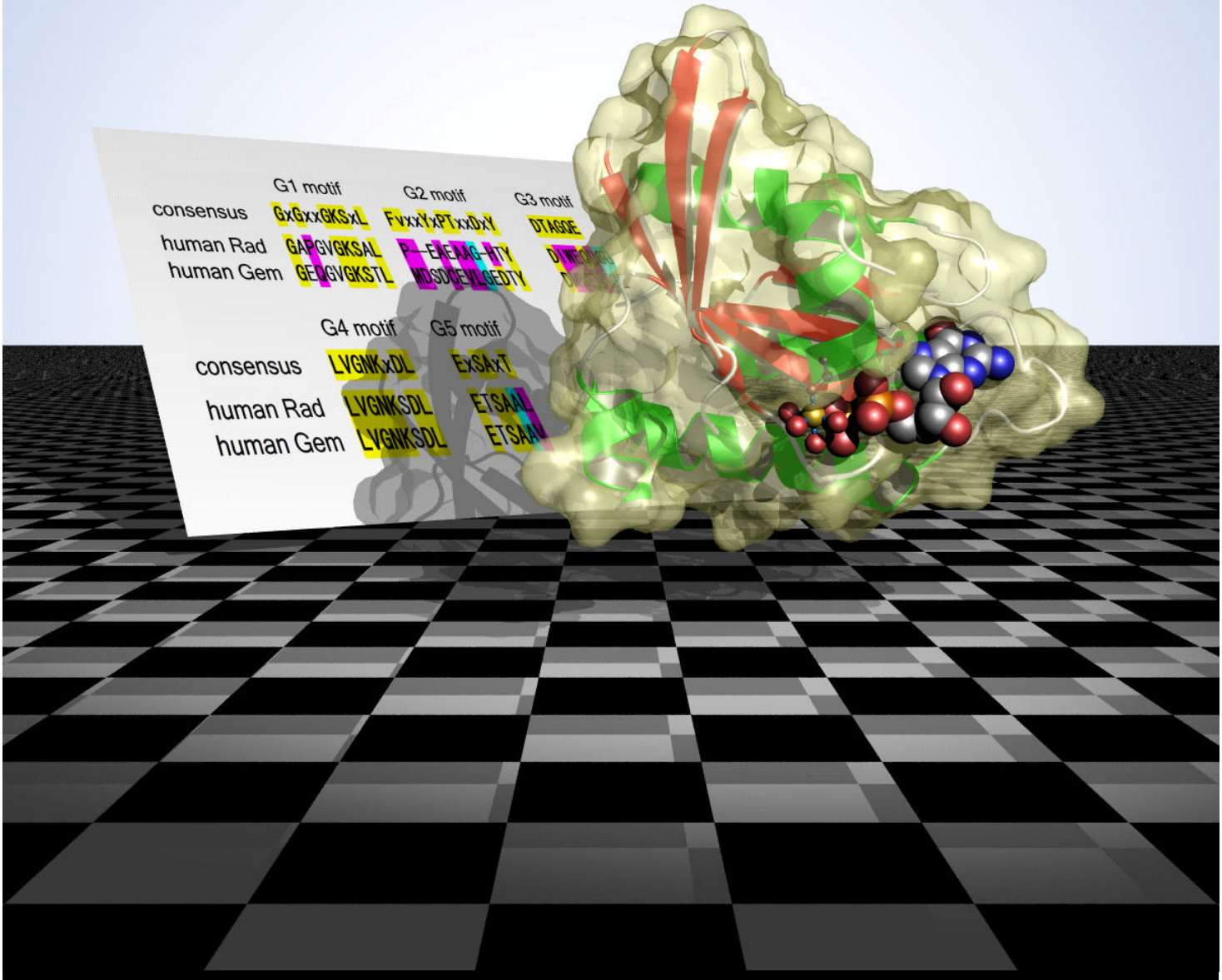

Laboratory of Structural Biology
Nara Institute of Science and Technology
August 28, 2006

Doctoral Dissertation

Structural characterization of human Rad GTPase of the RGK-family

Arry Yanuar

Laboratory of Structural Biology
Nara Institute of Science and Technology
August 28, 2006

Summary

Rad (Ras associated with diabetes) is an RGK-family small GTPase that is overexpressed in the skeletal muscle of humans with type II diabetes. Two conformation states behave as a binary switch cycling between the active GTP-bound form and the inactive GDP-bound form. The active GTP-bound form recognizes target proteins or effectors and trigger a response until the switch turn off to the GDP-bound form by GTPase activity. In principle, small GTPases possess a common GTPase domain that consists of about 170 residues with five conserved amino acid motifs, G1-G5, which are involved in GTP binding and hydrolysis and base recognition. Curiously, RGK family members including Rad lack several functionally important residues that are strictly conserved in the GTPase domains of other small GTPases.

In an effort to better understand the structure-function relationship of these novel GTPases, I have determined the first crystal structure of a member of the RGK-family GTPases, human Rad GTPase in complex with GDP at 1.8 Å resolution. The structure revealed unexpected disordered structures of both switch I and II regions. I showed that the conformational flexibility of both switches is caused by nonconservative substitutions in the G2 and G3 motifs forming the switch cores together with other substitutions in the structural elements interacting with the switches. Glycine-rich sequences of the switches would also contribute to the flexibility. Switch I lacks the conserved phenylalanine that makes nonpolar interactions with the guanine base in H-Ras. Instead, water-mediated hydrogen bonding interactions were observed in the Rad structure. The GDP molecule is located at the same position as in H-Ras and adopts a similar conformation as that bound in H-Ras. This

similarity seems to be endowed by the conserved hydrogen bonding interactions with the guanine base-recognition loops and the magnesium ion that has a typical octahedral coordination shell identical to that in H-Ras.

The conclusion is the structure of the GDP-bound form of Rad revealed uncommon structural features of the human Rad GTPase domain, especially conformational flexibility in the switch I region. These findings provide valuable clues for further biochemical and biomedical analyses of this novel small GTPase that is closely engaged in cytoskeletal rearrangement, ion channel regulation, diabetes and cancer

Contents

List of Figures

List of Tables

I. Introduction

Small GTPases regulate wide variety of cellular processes consisting intracellular signaling, vesicular transport, cytoskeletal rearrangement and nucleus transport (Herrmann 2003). These enzymes possesses two conformation state behave as a binary switches cycling between the active GTP-binding form and the inactive GDP-binding form. The active state GTP-binding form recognize target proteins or effectors and trigger a response until the switch turn off by GTP hydrolysis (Figure 1).

Rad (Ras associated with diabetes), is a new member of the small GTPase identified by subtractive cloning, is overexpressed in skeletal muscle of patients with type II diabetes mellitus (Reynet and Kahn 1993). Within Ras superfamily of small GTPases, Rad was included in a subfamily that has been given the name RGK together with Gem, Kir, Rem and Rem2 (Olson 2002). The human Rad gene was localized to chromosome 16q22 (Doria et al. 1995) encode 61% amino acid sequence identity to Gem (Maguire et al. 1994) and Kir (Cohen et al. 1994) containing five well conserved amino acid motif, G1-G5 that is highly related to other Ras GTPase superfamily.

Rad possesses a distinct structural feature among the Ras GTPase superfamily that might affect GTP binding or GTPase activity. Interestingly, Rad contains nonconserved residues within region G1, G2 and G3 of GTPase core domain. These region are known to be involved in GTP binding and GTP hydrolysis (Zhu et al. 1995).

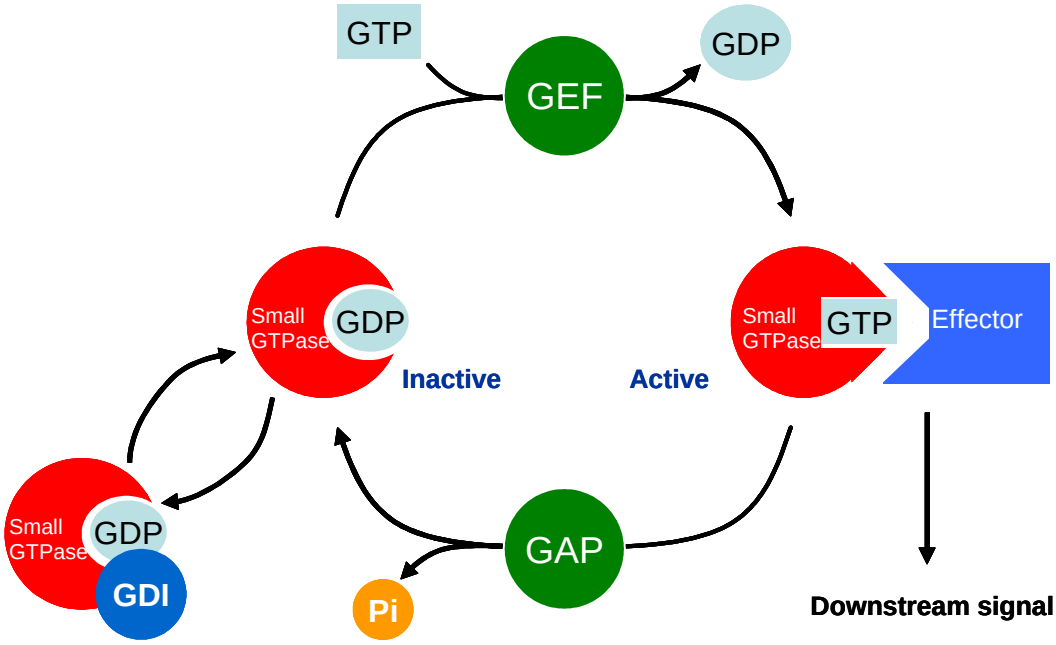

Figure 1. The small GTPase and its regulation.

Small GTPases cycling between GDP-bound and GTP-bound form. This cycle is regulated by GDIs, GEFs and GAPs. The GTP-bound form can recognize effector or target protein to give downstream signal.

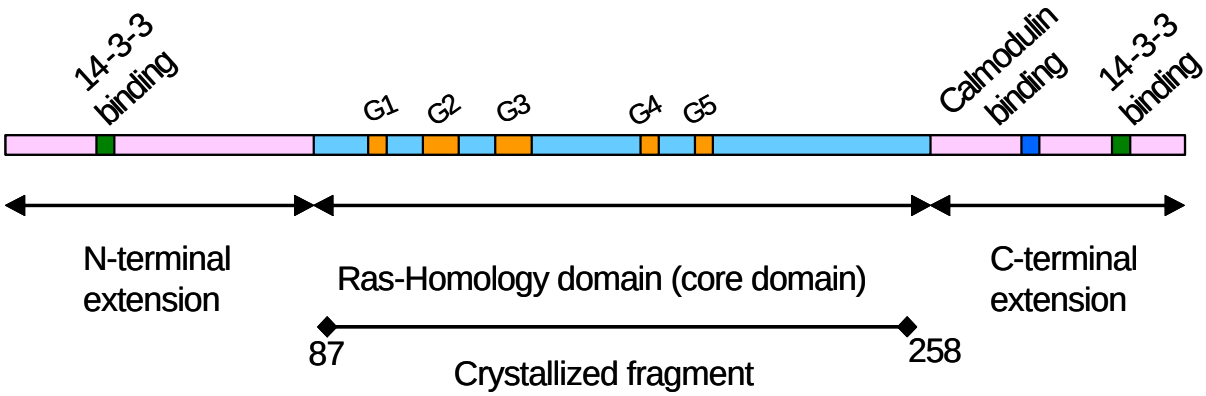

Figure 2. Structural feature of Rad GTPase.

GTPase domain (core domain) of human Rad GTPase is composed by 170 residues from 308 residues of the full length. Two 14-3-3 binding site are located at N- and C- terminal, while calmodulin binding site is only located in C-terminal. These N- and C-terminal were omitted for crystallization fragment.

Small GTPases possess a common GTPase domain that consists of about 170 residues with five conserved amino acid motifs, G1-G5, which are involved in GTP binding and hydrolysis and base recognition (Vetter and Wittinghofer 2001). The domain exists in two conformational states and behaves as a binary switch that cycles between the active GTP-binding and the inactive GDP-binding forms. The switch function is achieved by large conformation changes in two flexible regions refered to as switches I and II. Compared with other small GTPases, Rad has distinct features in the amino acid sequence, which might affect GTP binding or GTPase activity. The Rad GTPase core domain, which exhibits ~35% identity with other small GTPases such as H-Ras, contains crucial substitutions in the conserved motifs, G1-G3 and G4 (Zhu et al. 1995). In fact, recombinant Gem, Rad and Rem are known to display exceedingly low levels of intrinsic GTPase activity (Cohen et al. 1994; Zhu et al. 1995; Finlin et al. 2003).

Another notable characteristic of Rad is its N- and C-terminal extensions that consist of 85 and 50 residues, respectively. These extensions contain 14-3-3 and calmodulin binding sites (Moyers et al. 1997; Beguin et al. 2006) (Figure 2). Although Rad has 100% share of identity to Gem/Kir for 11 amino acids at COOH terminus (Moyers et al. 1997), it lacks the typical CAAX prenylation motifs needed for posttranslational modifications as shown in other Ras GTPase proteins (Takai et al. 2001). Expression of Rad in COS-1 cells induced dendrite-like extensions, and this protein was present at submembranous/cyto-plasmic regions and in the nucleus (Beguin et al. 2006).

Rad inhibits insulin-stimulated glucose uptake in myocyte and adipocyte cell lines (Moyers et al. 1996). Rad and its closely-related GTPases, Gem, Kir, Rem and Rem2, form an RGK subfamily in the Ras-family small GTPases (Olson 2002). These RGK-family members play three other important roles in cell biology (Kelly 2005). RGK GTPases function as potent inhibitors of voltage-dependent calcium channels (VDCCs) by direct binding to the *b*-subunit of VDCC (Beguin et al. 2001). Moreover, two members of the family, Gem and Rad, modulate Rho-dependent remodeling of the cytoskeleton by directly binding to Rho-kinases, leading to inhibition of kinase activity (Ward et al. 2002). A putative tumor suppressor, nm23-H1, was reported to convert Rad-GDP to Rad-GTP, in a manner akin to guanine-nucleotide exchange factors (GEFs) (Zhu et al. 1999), and regulate the growth and tumourigenicity of breast cancer (Tseng et al. 2001). Thus, Rad is a key GTPase that is involved in biologically and medically important processes.

In an effort to better understand the structure-function relationship of these novel GTPases, we have determined the first crystal structure of a member of the RGK-family GTPases, human Rad GTPase in complex with GDP at 1.8 Å resolution.

II. Material and Methods

Preparation and crystallization of Rad

Construct

Gene of GTPase core domain of human Rad protein encoding residues of 87-258 was cloned into glutathione-S-transferase (GST) and modified vector pPRO-EX (Invitrogen) with TEV protease cutting site at NH_2-terminal. The plasmid was transformed into and expressed in *Escherichia coli* strain BL21 star (Invitrogen).

Protein overexpression

Eschericia coli cells were grown in Luria Bertani media supplemented with ampicillin (100 μg ml^{-1}) at 310 K to an OD_{600} of 0.5. Expression of Rad was induced by the addition of isopropyl-*b*-D-thiogalactoside (IPTG) to 0.5 m*M*. Cells were cultured for 3 hours following induction at 310 K and then harvested by centrifugation at 6000 rpm for 15 min. Cells were washed with 0.9% NaCl, pelleted by centrifugation at 7000 rpm for 30 min and then resuspended in buffer A (300m*M* KCl, 2 m*M* $MgCl_2$, 5 m*M* DTT, 1% Triton X-100 and 50 m*M* Tris-HCl, pH 8.0) containing protease inhibitor. Cells were disrupted by sonication in an ice bath and the resultant cell suspension clarified by ultracentrifugation at 37K rpm for 30 min.

Protein purification

Purification of the protein was carried out by affinity chromatography using Glutathione Sepharose 4B (GSH-4B) (Pharmacia). The lysate supernatant was loaded onto the GSH-4B column equilibrated with buffer A. The resin was washed with 25 column volumes of buffer B (buffer A without Triton X-100). GST-fusion Rad bound to the resin

was digested in the column with 0.24 mg/ml His-TEV-protease for 3 hours at 293 K. The column was eluted with 6 volumes of buffer C (150 m*M* KCl, 2 m*M* $MgCl_2$, 5 m*M* DTT and 50 m*M* Tris-HCl, pH 8.0) and the effluent was passed through a Ni-NTA column (Qiagen) to remove the His-TEV-protease. The GST-free Rad was then concentrated by centrifugration using an Amicon Ultra-15 10,000 mwco (Amicon). The buffer was then changed to buffer D (50 m*M* KCl, 2 m*M* $MgCl_2$, 5 m*M* DTT and 50 m*M* Tris-HCl, pH 8.0) by HiPrep Desalting 26/10 (Pharmacia). SDS-PAGE (12.5%) analysis of the protein showed one major band corresponding to 19 kDa (Figure 3).

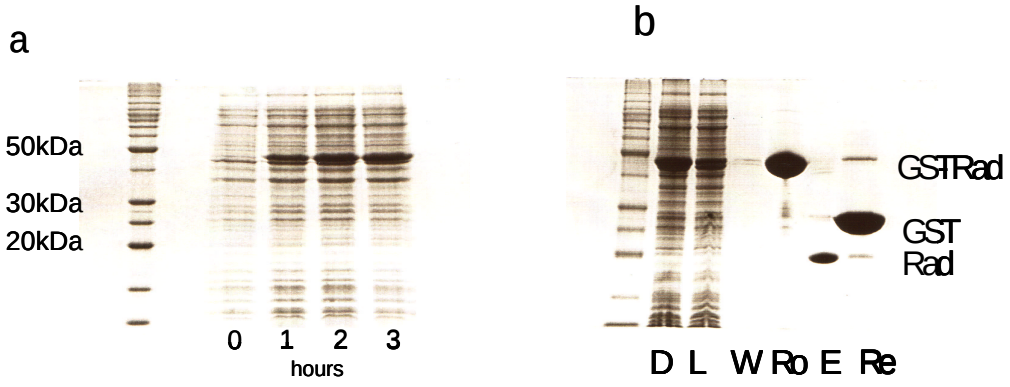

Figure 3. SDS PAGE analysis of human Rad GTPase

a. The GST-Rad fusion protein was expressed in *E. coli* (the major bands at 47 kDa.) within 3 hours at 310 K in LB media supplemented with ampicillin.

b. The GST-Rad fusion protein was purified using affinity chromatography with a GSH-Sepharose 4B column. The cells were disrupted (D) by sonication and loaded onto the colomn, the flowthrough was then collected (L). The column was then washed by the washing buffer and the flowthrough was then collected (W). The resin was then sampled before incubated (Ro) with TEV-protease for 3 hours. The resin was then eluted by the elute buffer (E) and the resin was checked in SDS PAGE (Re). The pure protein showed as a single major band in SDS PAGE after cutting GST tag by TEV-protease.

Wet cell was sonicated in sonication buffer.

↓

Ultracentrifuge 37000 rpm, 30 min, 277K

↓

The supernatant was loaded onto a GSH sepharose 4B column and washed

↓

The GST-tag was cleavaged with TEV protease, 3hr, 293K in the column

↓

A Ni-NTA column was used to remove TEV protease

↓

Hiprep Desalting

↓

Nucleotide exchange steps

Figure 4. Purification steps of human Rad GTPase

MonoQ Column I (Figure 6a)

↓

Alkaline phosphatase

↓

Hiprep Desalting

↓

MonoQ Column II (Figure 6c)

↓

Collect new peak

↓

Hiprep Desalting

↓

MonoQ Column III (Figure 6d)

↓

Collect the single peak of GTP analogue complex with Rad

Figure 5. Nucleotide exchange steps of human Rad GTPase

Nucleotide exchange

The exchanging a native nucleotide GTP or GDP with a nucleotide analogue was done according to the modified methods as described previously (Thompson et al. 1998). The GST-free Rad protein (about 0.3 m*M*) was incubated with 5 times excess molar ratio of each nucleotide analogue GTPγS, GMPPNP or GMPPCP (Sigma) and 30 unit of alkaline phosphatase (Sigma, P4439) for 1 hour at 310 K with gently mixing at 100 strokes per minute. The solution was then added by 20 m*M* $MgCl_2$ after reaction.

The solution was then loaded onto a HiPrep Desalting 26/10 column using buffer D to remove alkaline phosphatase and unbound nucleotides. The formation of the Rad-nucleotide complex was monitored and purified using FPLC with a MonoQ HR 10/100 GL column pack (Pharmacia) using linear gradient of salt from 50 to 300 mM KCl in 2 m*M* $MgCl_2$, 5 m*M* DTT, 50 m*M* Tris-HCl, pH 8.0 (Figure 6).

The samples Rad-GDP, Rad-GTPγS, Rad-GMPPNP, Rad-GMPPCP, were then concentrated to ~20 mg/ml using an Amicon Ultra-4 (Amicon) with 100 m*M* KCl, 2 m*M* $MgCl_2$, 5 m*M* DTT and 10 m*M* Tris-HCl, pH 8.0. The Rad complex with GMPPCP were partly precipitated during concentrating to ~20 mg/ml, thus it was in low concentration for crystallization process.

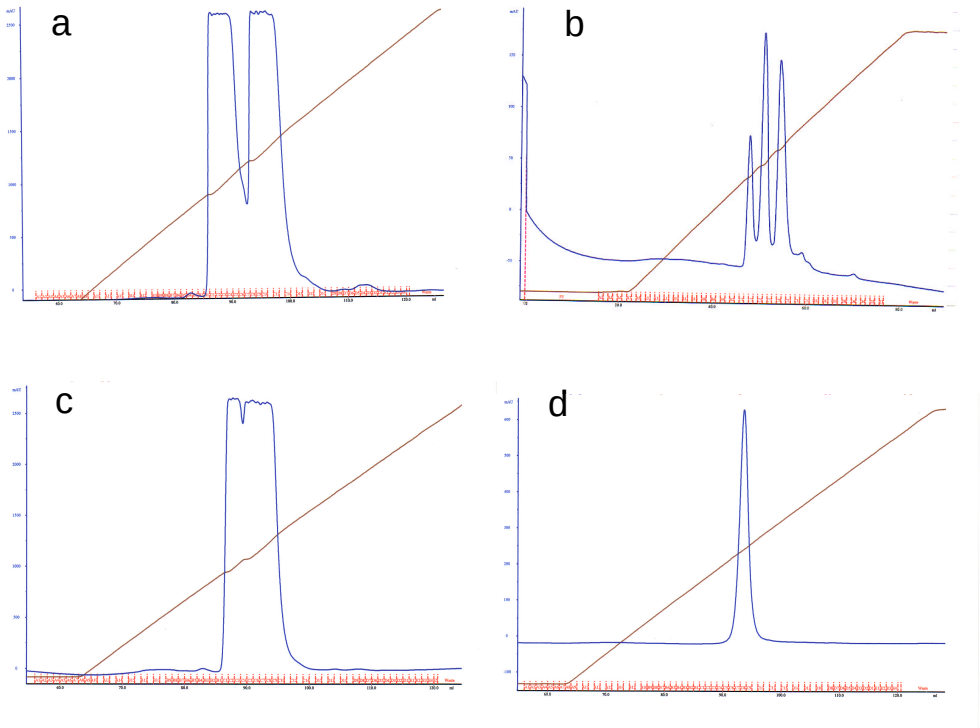

Figure 6. Nucleotide exchange monitoring

The nucleotide exchange experiments were performed with a MonoQ column HR 10/100 GL (Pharmacia). **(a)** The Rad protein after purification contains two peaks as a GDP-bound form (the first peak) and a GTP-bound form (the second peak). **(b)** Rad was exchanged with GMPPNP without separation of GDP-bound form and GTP-bound form or skip the MonoQ column I in Figure 5. The Rad GMPPNP-bound form was shown as a new peak at the middle position. **(c)** The GDP-bound form of Rad was exchanged with GMPPNP gave a new peak at the second position as Rad GMPPNP-bound form and **(d)** the GMPPNP-bound form of Rad was shown as a single peak correlated to the second peak in (b) or (c).

Gel filtration analysis

Gel filtration experiment were performed on a Superdex 75 26/60 HiLoad pg column. The molecular weight markers used was Gel Filtration Standard (BioRad) consisted of thyroglobulin (670 kDa, 5.0 mg), gamma globulin (158 kDa, 5.0 mg), ovalbumin (44 kDa, 5.0 mg), myoglobin (17 kDa, 2.5 mg), vitamin B-12 (1.35 kDa, 0.5 mg) diluted with 0.5 ml of deionized water. The molecular weight markers and Rad GTPase bound to GDP were eluted with the buffer containing 100 mM KCl, 50 mM Tris HCl pH 8, 2 mM $MgCl_2$, 5 mM DTT at flow rate 1 ml min^{-1}. The result of this analysis implies that a monomer state of the Rad GTPase in a solution (Figure 7).

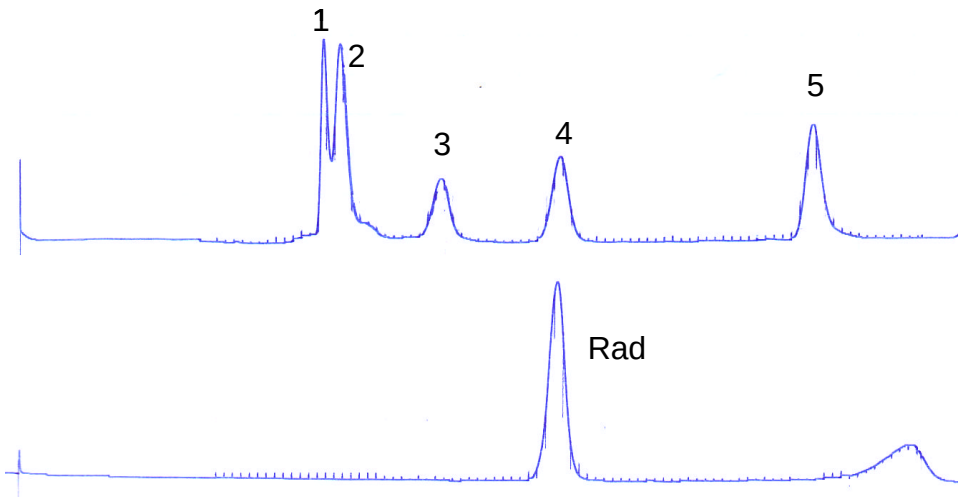

Figure 7. Gel filtration analysis of human Rad GTPase.

Rad protein is a monomer in the solution as shown at 19 kDa peak in the lower chromatogram. The upper chromatogram is the standard molecular weight consisted of (1) thyroglobulin (670 kDa, 5.0 mg), (2) gamma globulin (158 kDa, 5.0 mg), (3) ovalbumin (44 kDa, 5.0 mg), (4) myoglobin (17 kDa, 2.5 mg), (5) vitamin B-12 (1.35 kDa, 0.5 mg).

Crystallization

Crystallization screening was carried out by sitting drop methods using Nextal Biotechnologies screening kits. The Rad protein complex with GDP solution was mixed in a 1:1 ratio with the reservoir solution for 200 nl sitting drop volume and 100 μl reservoir solution using Hydra II crystallization robot (Matrix Technologies Corporation). Initial crystallization condition at 293 K using Sparse Matrix 3 (Nextal Biotechnologies) containing 100 m*M* MOPS pH 7.0, 20% PEG 3350, 100 m*M* $MgCl_2$ produced small stack of needle shape crystals. Optimization was carried out using hanging drop method by changing the pH, the PEG molecular weight and concentration and the magnesium chloride concentration, and by additionally using Additive Screen and Detergent Screen (Hampton Research, USA). Optimal crystal growth was achieved at 2- 3 days, 293 K in 4 μl hanging drop containing 100 m*M* MOPS pH 7.0, 25% PEG 3350, 25 m*M* $MgCl_2$, 10 m*M* DTT as a precipitant in a 1:1 volume ratio with 11 mg ml^{-1} protein solution and 500 μl of 100 m*M* MOPS pH 7.0, 21% PEG 3350, 25 m*M* $MgCl_2$, 10 m*M* DTT as reservoir solution (Figure 8).

Although the Rad-GDP complex was succeeded to be crystallized, the Rad complex with each GTP analogue such as GTPγS and GMPPNP was failed to form a good crystal in the various screening conditions.

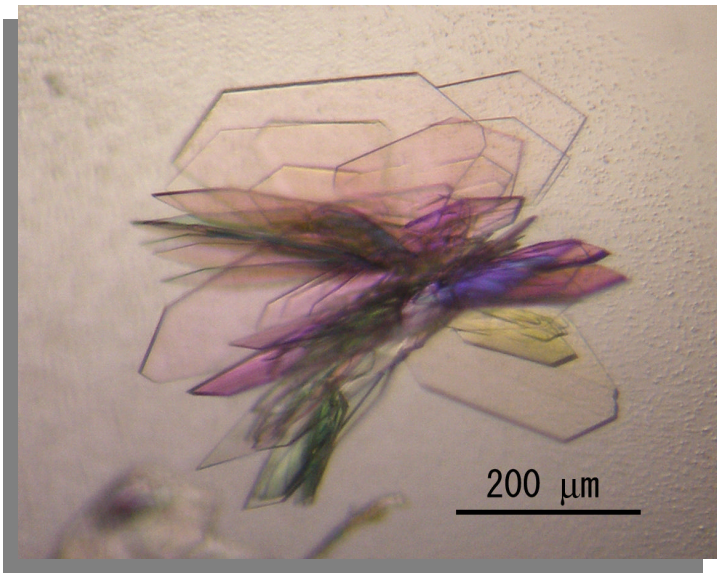

Figure 8. The crystal of human Rad GTPase.

The crystal was developed for 2-3 days at 293 K in 100 m*M* MOPS pH 7.0, 25% PEG 3350, 25 m*M* $MgCl_2$, 10 m*M* DTT using vapour diffusion hanging drop methods.

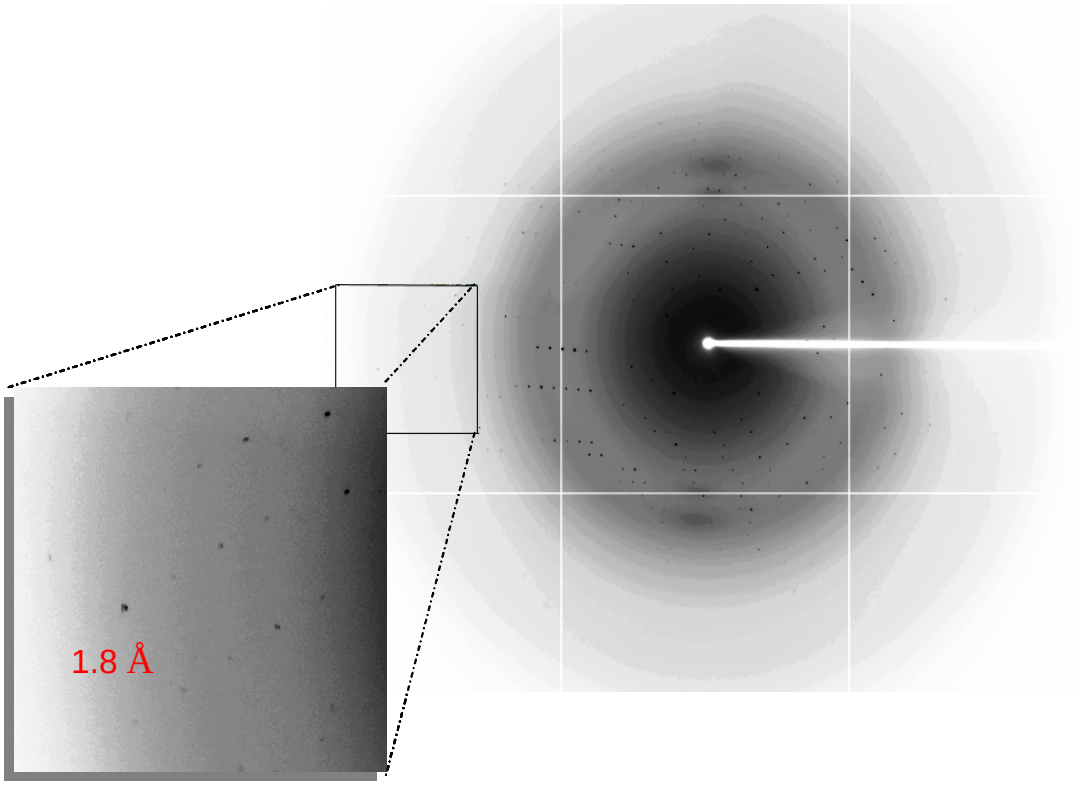

Figure 9. X-ray diffraction image of human Rad GTPase crystal at 1.8 Å.

A diffraction data set was collected to a resolution of 1.8 Å at collected at SPring8, Japan, on beamline BL41XU using ADSC Quantum 315 CCD detector system.

X-ray diffraction data collection

Cryogenic preparation

Crystals were transferred into cryoprotectant solution containing 20%(v/v) glycerol in crystallization solution, mounted on nylon loop and flash-frozen in liquid nitrogen to prevent ice lattice formation in the aqueous medium.

Data collection

An X-ray diffraction data for Rad crystal was collected at SPring8, Japan, on beamline BL41XU using ADSC Quantum 315 CCD detector system (Table 1). The wavelength was set to 1.0 Å. The crystals were maintained at a temperature of 100 K during data collection. A diffraction data set was collected to a resolution of 1.8 Å (Figure 9). Diffraction data were indexed, integrated and scaled using the *HKL2000* program suite (Otwinowski and Minor 1997). The crystals were found to belong to space group $P2_1$, with unit-cell parameters *a*=52.2, *b*=58.6, *c*=53.4Å, *b*=98.0° (Table 2).

Each intensity, I (*h k l*), of data was then evaluated from images and transformed to amplitude of structure factor, **F** (*h k l*). We observed 97,986 reflections containing 28,220 unique reflections with completeness 94.6 % and R_{merge} 6.6 %. The reliability factor of the data, R_{merge}, is defined by,

$$R_{merge} = \frac{\sum \mid Ii(h\,k\,l) - \langle I(h\,k\,l)\rangle \mid}{\sum Ii(h\,k\,l)}$$

Where Ii(*h k l*) is the i^{th} measurement and <I(*h k l*)> is the mean of the measurement of the reflection. The typical value of R_{merge} is under 10 %.

An estimation of the number molecules per unit cell, Z, can be made by a V_M value which is the ratio of the unit cell volume and the molecular weight (Matthews 1968). The V_M value is given by,

$$V_{\mathrm{M}} = \frac{V_{cell}}{M_{\mathrm{r}} Z}$$

where V_{cell} is the the volume of the unit cell and M_w is the molecular weight of the protein. V_M value is usually range between 1.7 and 3.5 $Å^3Da^{-1}$ for protein crystals. The human Rad GTPase crystal was estimated to contain two molecule in the asymmetric unit and two asymmetric unit per unit cell (Z=4) with V_M value 2.1 $Å^3Da^{-1}$. The solvent content of the crystal, V_{solv}, is calculated from V_M values by,

$$V_{solv} = 1 - \frac{1.23}{V_{\mathrm{M}}}$$

and this calculation gave 42 % solvent content for the human Rad GTPase crystal. A summary of the crystal data is given in Table 2 and a summary of the intensity data processing is given in Table 3.

Structural determination and refinement

Molecular replacement

Structure factor **F** (*h k l*) as a Fourier transform of electron density *r* (*x y z*) can also be transformed back to get electron density using the same transformation method.

$$\rho(x\ y\ z) = \frac{1}{V} \sum_h \sum_k \sum_l \mathbf{F}(h\ k\ l)\ e^{-2\pi i(hx+ky+lz)}$$

where *x*, *y*, and *z* are relative coordinates in the real space unit cell, and *h*, *k*, and *l* are the reciprocal lattice point. Because

$$\mathbf{F}(h\ k\ l) = \mid F(h\ k\ l) \mid \ e^{i\alpha(h\ k\ l)}$$

then the previous equation can also be written as :

$$\rho(x\ y\ z) = \frac{1}{V} \sum_{h} \sum_{k} \sum_{l} \mid F(h\ k\ l) \mid \ e^{-2\pi i(hx+ky+lz)+i\alpha(h\ k\ l)}$$

and |*F (h k l)*| is derived from the intensity *I (h k l)*

$$\mid F(h\ k\ l) \mid^2 = I(h\ k\ l)$$

but phase angle *a (h k l)* remain to be determined because it cannot be obtained directly from diffraction pattern.

The result of X-ray diffraction experiment give only the amplitudes of structure factor, **F**(*h k l*). To build the electron density, the phase angle of structure factors, *a*?(*h k l*), are required. The phase could be determined using several methods such as molecular replacement, multiwavelength anomalous dispersion, or isomorphous replacement. Molecular replacement method (Rossmann and Blow 1962) can be performed if the protein structure or its homologous has already been discovered. If there is no homologous protein is established or the protein is the first time to be crystallized, the heavy atom derivative method can be applied for obtaining phase using multiwavelength anomalous dispersion or isomorphous replacement.

In most cases of successful molecular replacement application, the sequences of protein of interest and of the structural homologue are at least 35 % identical. (Claude et al.

2004). Using the program *MODELLER* (Sali and Blundell 1993), starting models for molecular replacement was obtained by homology modeling with Ras-family GTPases, H-Ras (PDB code 1JAH), Rap1A (1GUA), Rap2 (3RAP) and RalA (1U90 and 1UAD). These GTPases exhibit between 34-37% sequence identity with Rad. The structural analysis was carried out using polyalanine models with the molecular replacement program *MOLREP* (CCP4 (Collaborative Computational Project) 1994; Vagin and Teplyakov 1997). The orientation and position of the molecule in the target unit cell were determined using rotation and translation function (Crowther and Blow 1967; Crowther 1972) The model was refined using six parameters, three rotations and three translations. The correct solution should give the small value of reliability factor and high value of correlation coefficient.

Reliability of the solution in the molecular replacement methods are determined by R_{factor} or R_{cryst} or (R) and the correlation coefficient (C) as followed,

$$R = \frac{\sum_{hkl} || \mathbf{F}_{obs} | - k | \mathbf{F}_{calc} ||}{\sum_{hkl} | \mathbf{F}_{obs} |}$$

k is the scale factor between observed and calculated structure factor. It is calculated with

$$k = \frac{\sum_{hkl} | \mathbf{F}_{obs} || \mathbf{F}_{calc} |}{\sum_{hkl} (| \mathbf{F}_{calc} |)^2}$$

and

$$C = \frac{\sum_{hkl}(|\mathbf{F}_{obs}|^2 - \overline{|\mathbf{F}_{obs}|^2})(|\mathbf{F}_{calc}|^2 - \overline{|\mathbf{F}_{calc}|^2})}{\left[\sum_{hkl}(|\mathbf{F}_{obs}|^2 - \overline{|\mathbf{F}_{obs}|^2})^2 \sum_{hkl}(|\mathbf{F}_{calc}|^2 - \overline{|\mathbf{F}_{calc}|^2})^2\right]^{1/2}}$$

Both values, R and C, gave the agreement index between calculated structure factors, F_{calc}, and observed structure factors, F_{obs}.

Electron density map and model building

Fourier coefficient from the experiment was improved for generating map using the calculated phases from partially known structure using the program SIGMAA (Read 1986; CCP4 (Collaborative Computational Project) 1994). Prime-and-switch phasing was performed to remove model bias using the program *RESOLVE* (Terwilliger 2003) prior to creating (2Fo-Fc) electron denstity maps. Density modification with solvent flattening, histogram matching and non crystallographic symmetry averaging was also performed to improve electron density maps. Model building was performed using the program *O* (Jones and Kjeldgaard 1997). Difference Fourier maps were calculated for model building of the bound GDP molecules and picking magnesium ions (Figure 18).

Refinement

The structure was refined with the *CNS* program (Brünger et al. 1998). Non crystallographic symmetry was treated during the refinement process until an *R* value of 31.7% (an R_{free} of 32.0 %) was achieved. At this stage water molecules were then introduced to the structure. After several cycles of refinement, the structure was refined with an *R* value of 21.4% (an R_{free} of 24.0%) without any residues in disallowed regions as checked by the program *PROCHECK* (Laskowski et al. 1993) to produce Ramachandran plot (Figure 11).

The results of the refinement of the structure are summarized in Table 6. The structure was inspected and rendered using the program *PyMOL* (DeLano and Bromberg 2004).

The atomic coordinates and structure factors have been deposited under accession code 2DPX in the Protein Data Bank (Berman et al. 2000).

Table 1. X-ray diffraction data collection condition of human Rad GTPase.

Beamline	SPring-8 / BL41XU
Detector	ADSC Quantum 315 CCD
Wavelength (Å)	1.00
Temperature (K)	100
Oscillation range (°)	180 (1.5° × 120 images)
Exposure time (seconds)	30

Table 2. Crystal data of human Rad GTPase.

Crystal System	Monoclinic
Space group	$P2_1$
Unit cell parameters	a = 52.2 Å, b = 58.6 Å, c = 53.4 Å;
	$a = g = 90$; $b = 98.0^o$
Unit cell volume ($Å^3$)	159958.0
Matthew's coefficient, V_M	2.1 $Å^3Da^{-1}$
Molecule in unit cell, Z	4
Molecule in asymmetric unit	2
Solvent content, V_{solv}	42 %
Mosaicity	0.3 – 0.5

Table 3. Intensity data processing of human Rad GTPase.

Resolution range (Å)[1]	50 - 1.80 (1.86 – 1.80)
Total reflections	97,986
Unique reflections	28,220
Completeness (%)	94.6 (72.2)
Mean $< I / (\sigma I) >$	12.4 (2.2)
R_{merge} (%)[2]	6.6 (44.4)

[1] Statistics for the outer resolution shell are given in parentheses.

[2] $R_{merge} = \Sigma \mid I_i - < I_i > \mid / \Sigma < I_i >$, where I_i is the observed intensity and $< I_i >$ is the average intensity over symmetry equivalent measurements.

Table 4. Solution of rotation and translation function for Rad GTPase.

$P2_1$

First Molecule (A)

Sol_ RF TF		θ	ϕ	χ	tx	ty	tz	R	C
Sol___1___1	1	49.39	149.17	110.89	0.495	0.000	0.322	0.578	0.265
Sol___2___1	2	62.20	129.95	91.36	0.883	0.000	0.196	0.583	0.247
Sol___4___1	3	46.22	139.82	90.52	0.181	0.000	0.135	0.603	0.199
Sol___5___4	4	61.35	137.71	101.15	0.873	0.000	0.190	0.597	0.194
Sol__10___1	5	30.04	-88.60	173.75	0.832	0.000	0.239	0.606	0.193
Sol___9___2	6	51.75	140.92	113.55	0.129	0.000	0.457	0.605	0.192
Sol___7___1	7	123.97	-114.23	117.00	0.120	0.000	0.315	0.606	0.190
Sol___6___5	8	103.59	-5.24	83.47	0.856	0.000	0.304	0.602	0.189
Sol___3___2	9	118.19	-33.53	68.63	0.894	0.000	0.295	0.605	0.174
Sol___8___8	10	21.15	-164.84	131.95	0.039	0.000	0.272	0.611	0.166

Second Molecule (B)

Sol_ RF TF		θ	ϕ	χ	tx	ty	tz	R	C
Sol___2___1	1	62.20	129.95	91.36	0.881	0.431	0.196	0.530	0.382
Sol___7___1	2	123.97	-114.23	117.00	0.120	0.942	0.812	0.567	0.305
Sol___5___1	3	61.35	137.71	101.15	0.878	0.444	0.189	0.573	0.280
Sol___4___3	4	46.22	139.82	90.52	0.682	0.809	0.135	0.585	0.256
Sol___6___6	5	103.59	-5.24	83.47	0.806	0.495	0.114	0.580	0.256
Sol__10___8	6	30.04	-88.60	173.75	0.789	0.432	0.282	0.584	0.256
Sol___9___1	7	51.75	140.92	113.55	0.969	0.292	0.838	0.591	0.243
Sol___3___9	8	118.19	-33.53	68.63	0.897	0.757	0.797	0.584	0.241
Sol___8___8	9	21.15	-164.84	131.95	0.094	0.706	0.715	0.585	0.240
Sol___1___8	10	49.39	149.17	110.89	0.000	0.615	0.817	0.649	0.224

The first ten of molecular replacement solutions for rotation and translation from Molrep for two molecules of Rad protein in the asymmetric unit. (θ, ϕ, χ) are polar angle and tx, ty, tz are the fraction of unit cell axes.

Table 5. Statistics of molecular replacement process.

Maximum resolution (Å)	3
Minimum resolution (Å)	
Rotation function	9
Translation function	9
Search radius (Å)	35
Molecule A	
Rotation (θ, ϕ, χ)*	49.39; 149.17; 110.89
Translation (tx, ty, tz)*	0.495; 0.000; 0.322
R_{cryst}	0.578
Correlation coefficient	0.265
Molecule B	
Rotation (θ, ϕ, χ)*	62.20; 129.95; 91.36
Translation (tx, ty, tz)*	0.881; 0.431; 0.196
R_{cryst}	0.530
Correlation coefficient	0.382

* Polar angles (θ, ϕ, χ) and fractional coordinate (tx, ty, tz) as defined in MOLREP

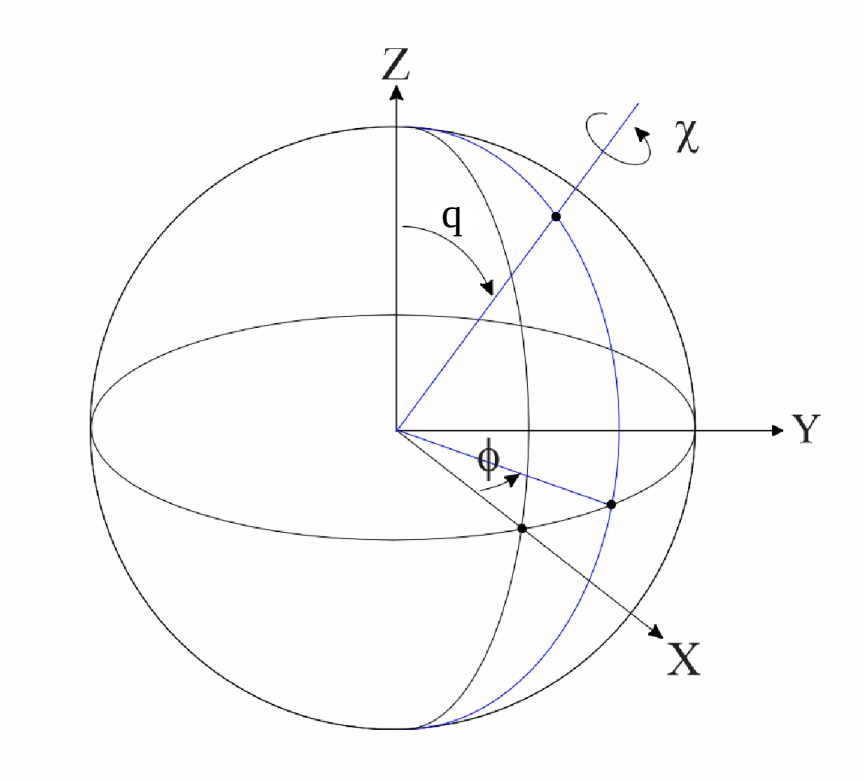

Figure 10. Polar angle q**,** f**,** c**.**

A direction of a molecules is shown using three polar angle (θ, ϕ, χ). This system is useful for detecting non-crystallographic symmetry. θ and ϕ determine the position of the rotation axis and χ is the rotation around this axis.

Table 6. Refinement statistics.

Resolution range (outer shell) (Å)	35 - 1.80 (1.91 – 1.80)
Number of reflections	26,737
R_{cryst} (%)	21.42
R_{free} (%)*	24.01
r.m.s. deviation from ideality	
Bond lengths (Å)	0.0087
Bond angles (°)	1.37
Dihedral angles (°)	23.8
Improper angles (°)	0.76
Average temperature factors (Å^2)	40.0
Molecule A / GDP / Mg^{2+}	37.3 / 25.4 / 24.3
Molecule B / GDP / Mg^{2+}	43.5 / 27.4 / 35.3
Water	39.6
Number of nonhydrogen atoms	
Protein	2,135
Nucleotide	56
Number of magnesium ions	2
Number of water molecules	83

* Free R factor is calculated from a randomly chosen subset of reflections not used for refinement.

Table 7. Ramachandran statistics.

Most favoured regions (%)	90.7
Additional allowed regions (%)	9.3
Generously allowed regions (%)	0

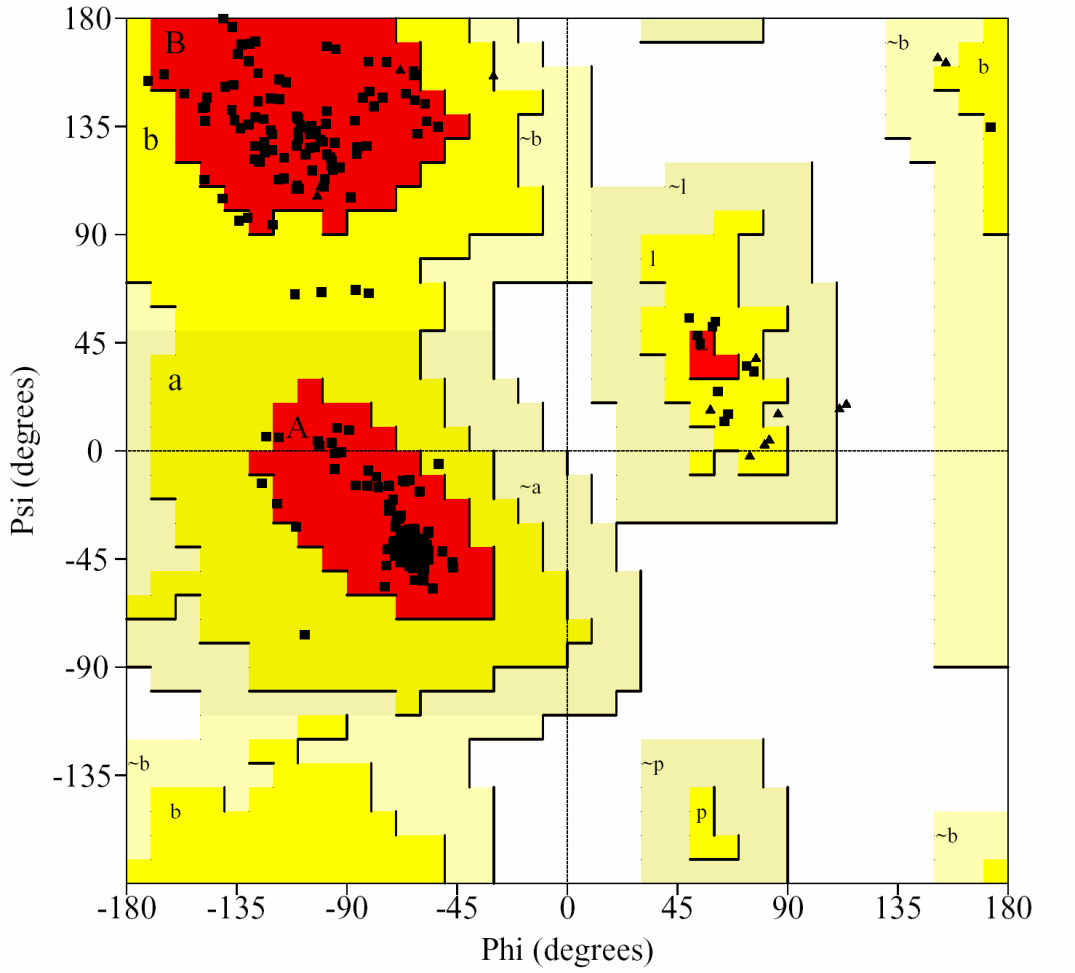

Figure 11. Ramachandran plot of crystal structure of human Rad GTPase.

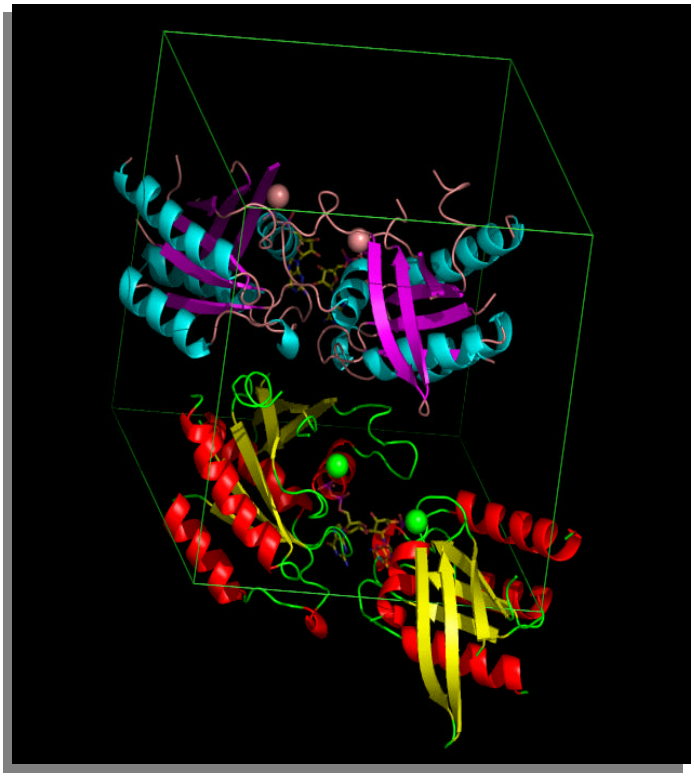

Figure 12. Crystal packing of human Rad GTPase in $P2_1$ monoclinic crystal system.

The crystal packing of the human Rad GTPase in $P2_1$ space group contains four molecules in the unit cell. There are two molecules in asymmetric unit designated as molecule A and B. The same color represents the asymmetric unit.

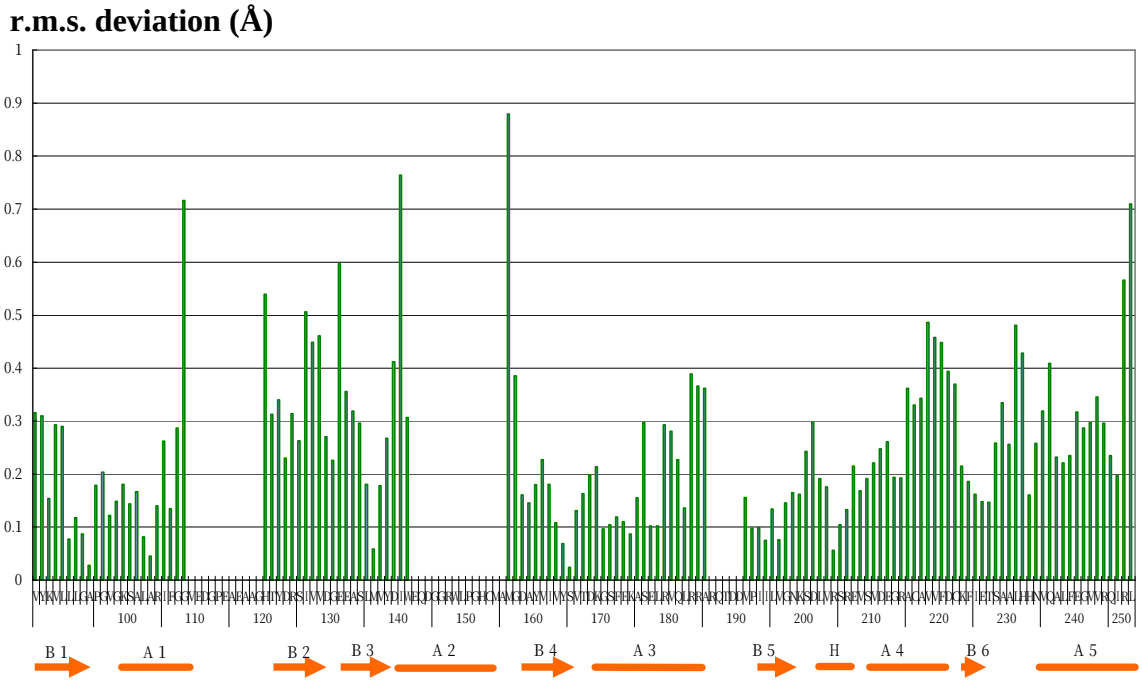

Figure 13. Root mean square deviation between molecule A and B of Rad GTPase.

The vertical axis is root mean square deviation in Å and the horizontal axis is residue with the number. The orange bars and arrows represent the secondary structure. Overall r.m.s deviation between two molecules is 0.3 Å. The missing part in the graph is the disordered region in one or both molecules that could not be compared for r.m.s.d.

III. Results

Overall structure

The crystal contains two Rad molecules, molecules A and B, in the crystallographic asymmetric unit of a $P2_1$ crystal lattice (Figure 12). These two molecules form a dimer in the crystal lattice, though Rad exists as a monomer in solution, confirmed by gel filtration giving a single peak at 19 kD (Figure 7). The structure of these two molecules is essentially the same with a small root mean square (r.m.s.) deviation of 0.30 Å (Figure 13). Rad contains five α-helices (A1-A5) and one large β-sheet that comprises two extended anti-parallel β-strands (B2 and B3) and five extended parallel β-strands (B3, B1, B4-B6) (Figure 15).

These major features of the Rad GTPase domain fold are basically conserved as found in H-Ras and other related small GTPases, consisting of a six-stranded β-sheet surrounded by helices connected with loops. The bound GDP molecule was found at the canonical nucleotide-binding site (Figure 18). The current model contains three poorly-defined loop regions, switches I and II and loop A3-B5, which were omitted from the model (Figure 14 and 10). Excluding residues of poorly defined loops and altered helix A2, the C_α-carbon atoms of Rad when superimposed on the GDP-bound forms of H-Ras (Tong et al. 1991) and RalA (Nicely et al. 2004) yield relatively small r.m.s. deviations of 0.79 Å and 0.86 Å for 124 and 128 C_α-carbon atoms, respectively (Figure 16). Thus, the Rad GTPase domain displays no significant changes in the overall fold compared to H-Ras and other Ras-family GTPases such as RalA, though there are several unusual features in the detailed structures which will be described below.

The switch I region

The switch I region of small GTPase generally contains the G2 motif (FVXXYXPTXXDXY where X represents any amino acid residue) that is important for nucleotide binding. The Rad switch I region, however, lack this motif (Figure 14). In the crystal, switch I was disordered and most of the residues are invisible in the current map (Figure 19a). Helix A1, which is followed by switch I, is important for stabilization of the switch I conformation. Helix A1 of Rad is shorter than that of H-Ras, being hampered by two glycine residues (112 and 113) at the C–terminus of the helix. These small residues cause a small shift in the C-terminal part of helix A1 toward the β-sheet (Figure 19a). In H-Ras, Ile24 exist at the position corresponding to Gly112 of Rad and stabilizes helix A1 by making contacts with the β-sheet (Figure 19b). In addition to these changes in configuration, Rad helix A1 has a polar residue, Arg109, on helix surface. This position is usually occupied by a nonpolar residue, Ile21 in H-Ras, which stabilized the loop conformation of switch I through hydrophobic interactions with two conserved residues, Val29 and Tyr32, of the G2 motif. Moreover, a hydrogen bond between conserved tyrosine residues Tyr32 and Tyr40 stabilizes the loop. The absence of the conserved valine and tyrosine residues, together with the relatively high content of mobile glycine residues, might impart flexibility to the Rad switch I region.

Rad switch I lacks the conserved phenylalanine (Phe28 of H-Ras) that traps the GDP molecule through non-polar interactions with the base and sugar. Instead, Arg109 on helix A1 serves to hold the nucleotide by forming a water mediated hydrogen bonding network (Figure 19a). Gem also lacks the conserved phenylalanine, which is replaced by Met102, while the entire amino acid sequence of the Gem switch I region is distinct from that of Rad (Figure 14). Interestingly, Gem also displays disordered switch I in the recently

reported crystal structure of the GDP-bound form of Gem (PDB ID 2G3Y, unpublished) (Figure 20b).

The switch II region

Switch II of Rad is disordered in the crystal, suggesting conformational flexibility. The G3 motif comprises the N-terminal half of switch II. Rad possess marked substitutions within this motif (D**IWE**Q**D**) compared to the common sequence (DTAGQE) that is completely conserved in H-Ras and RalA. At the beginning of the loop, two hydrophobic residues, Ile145 and Trp146, of Rad pack against helices A2 and A3 to form a compact hydrophobic cores (Figure 21a). Ile145 interact with Met161, which would result in unwinding of the C-terminus of helix A2. These interactions seem to induce a shift in orientation of helix A2 compared with that found in H-Ras (Figure 21b). Rad displays a similar orientation of helix A2 to that of RalA, though the length of the helix is a much shorter than that of RalA (Nicely et al. 2004). However, switch II of Gem appear as a long helices with 10 residues from K136 to H145 with new orientation and shifted to the N-terminal of the loop (Figure 22b). This difference in helix length is cause by the introduction of a helix breaker, Pro155, at the N-terminus of Rad helix A2.

At the middle of switch II, Rad contains two glycine residues, which would endow the loop with conformational flexibility. Switch II of H-Ras is stabilized by a salt bridge between Arg68 of the loop and Glu37 of switch I. These residues are not conserved in Rad, which might contribute to the flexibility. Rad preserves Gln148 (Gln61 of H-Ras, DTAG**Q**E) that is essential for catalytic activity in H-Ras and other small GTPases. However, it is suspected that the catalytic mechanism of GTP hydrolysis by Rad might be somewhat different from that of H-Ras. Indeed, mutation of Rad Gln148 had no effect on

GTPase activity (Zhu et al. 1995). Consistent with this, the corresponding residues are asparagine and alanine in Gem and Rem, respectively. This observation suggests that the conformational properties of Rad switch II are distinct from that of H-Ras and its closely-related GTPases.

The phosphate-binding loop

The phosphate-binding loop of Rad possesses a G1 motif (GX**P**XXGKSXL) that has a proline substitution, Pro100, at the second conserved glycine residue (G12 of Ras) of the common G1 motif (GX**G**XXGKSXL) (Figure 14). The location of this glycine residue is well known for the site of mutation to produce a transforming form of H-Ras. The crystal structure of mutated H-Ras GTPases shows that the mutations cause no significant conformational change in the phosphate-binding loop. Similar results were obtained in Rad, which displays the G1 motif well overlaid on those of H-Ras and RalA with extremely small r.m.s. deviation (0.16-0.18 Å) (Figure 23). This structural conservation is coincident with the fact that the Rad phosphate-binding loop retains main-chain interaction with β-phosphate of GDP as in H-Ras.

In H-Ras, several bulky mutation of Gly12 such as G12V and G12P are known to stabilize the switch II conformation through direct contact between the mutated bulky residue and switch II, and to define a single conformation of switch II, whereas wild-type H-Ras possesses a disordered switch II region (Krengel et al. 1990; Pai et al. 1990). A similar result was obtained for G14V mutation in RhoA (Ihara et al. 1998). Contrary to these observations, the Rad phosphate-binding loop with the Pro100 substitution might not contribute to stabilization of the switch II conformation. Perhaps the conformational

properties of Rad switch II are distinct from that of H-Ras as mentioned above. Mutation of Rad Pro100 to a glycine residue had no effect on GTPase activity (Zhu et al. 1995).

In Gem, the β-phosphate oxygen in the GDP molecule is stabilized by Ser89 and Asp31 through a water-mediated hydrogen bonding network (Figure 20).

Magnesium ion binding

In the Rad-GDP complex, the magnesium ion is located at the same position as in the H-Ras-GDP complex. The superposition of Rad and H-Ras proteins yields a small deviation of 0.37 Å for magnesium ions. The ion possesses the same octahedral coordination shell that includes four water molecules, one *b*-phosphate oxygen atom and the side chain of Ser105 (Ser17 of H-Ras) (Figure 21). Conserved Ser105 is located in the G1 motif and is stabilized by conserved Asp144 (Asp57 of H-Ras) of the G3 motif. Mutation of Ser105 with asparagine in Rad abolishes GTP binding (Zhu et al. 1995). Taking into account the lack of switch I-nucleotide interaction as in H-Ras, the magnesium ion seems to be more critical for GDP binding to Rad than in other GTPases. Interestingly, there is no magnesium ion present in the Gem GDP-bound form and also only two water molecules were found near the β-phosphate of GDP or around the magnesium ion position where usually four water molecules participate in Rad and H-Ras, suggesting nucleotide binding in Gem is weak. (Figure 20)

Moreover, switch I of Rad lack the conserved threonine residue (Thr35 of H-Ras) that is well known to coordinate to the magnesium ion in GTP-bound form, suggesting relatively weak binding of the magnesium ion to the GTP-bound form. This idea is consistent with the fact that Rad displays unique magnesium dependence where GDP and

GTP binding were optimal at relatively high magnesium ion concentrations (1-10 mM) (Zhu et al. 1995).

The base recognition

The GDP molecule bound to Rad displays an *anti* glycosyl conformation with a C2'-*endo* sugar pucker, basically identical to that of GDP conformations bound to other small GTPases including H-Ras. The guanine base is trapped in a hydrophobic pocket, in a manner similar to H-Ras, and participates in several interactions with conserved residues (Asn203, Lys204, Asp206 and Ala234) of the G4 and G5 motifs (Figure 24a). The hydrogen bonding network between the base and these two motifs is the same as in H-Ras. The superposition of Rad on H-Ras yields an r.m.s deviation of 0.95 Å for atoms of the bound GDP molecules. A notable difference in the base recognition site might be pointed out in the conformational stability of the G5 motif, in addition to the absence of contact with the conserved phenylalanine (Phe28 of H-Ras) in switch I as mentioned above. The Rad G5 motif (ETSAA**L**) replaces the conserved threonine residue (EXSAX**T**) with a leucine residue, Leu 236. In H-Ras and other small GTPases, the conserved threonine residue (Thr148 of H-Ras) plays an important role in stabilizing the base recognition loop of the G5 motif by forming intraloop hydrogen bonds (Figure 24b). Moreover, H-Ras possesses a lysine residue at the variant position of the G5 motif (ETSA**K**T), while Rad possesses an alanine residue at this site. This lysine residue of H-Ras, Lys147, forms a hydrogen bond to Asp119 and contributes to stabilization of the side-chain conformation of Asp119 that participates in guanine base recognition. The absence of these interactions in Rad might impart greater flexibility in the base recognition site formed by the G4 and G5 motifs. This

might be related to the observation that GTP binding to Rad was slightly inhibited in the presence of high ATP concentrations (Zhu et al. 1995).

Gem also gives the similar situation to that found in Rad. The base recognition loops of Gem show the same conformation of residues in G4 and G5 that take part in binding to the guanine base (Figure 25). Moreover, the GST-Kir protein showed GDP binding activity with an estimated K_d of 7 mM, lower affinity than that of Ras proteins (10 nM) (Cohen et al. 1994).

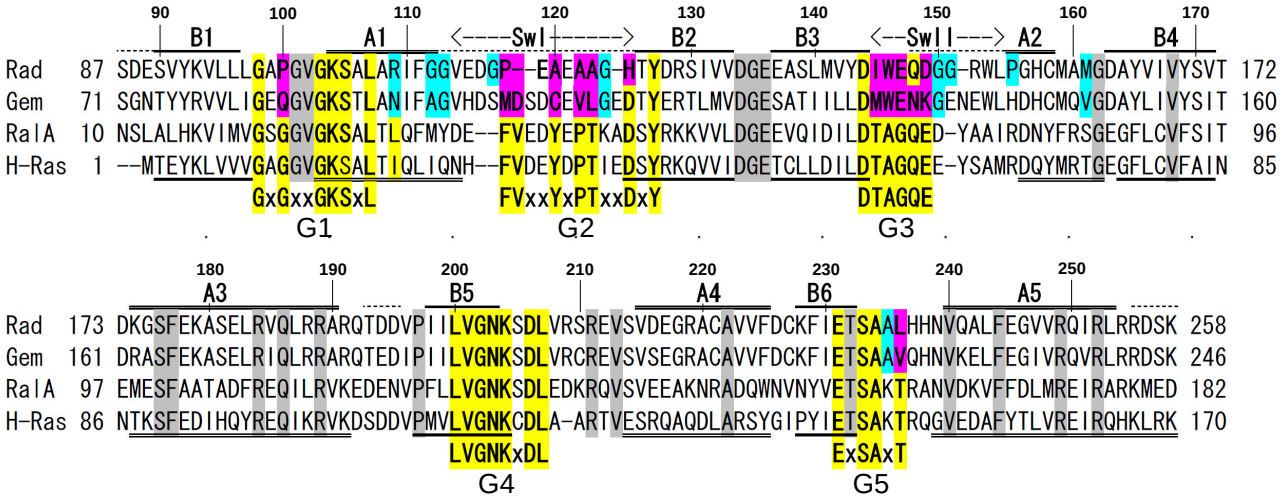

Figure 14. Sequence alignment of human Rad, Gem, RalA and H-Ras.

Secondary structural elements of Rad and H-Ras are indicated at the top and below, respectively. Omitted regions of the current Rad model comprise nine residues (116-124) in switch I, seven residues (147-153) in switch II, three residues (192-194) in loop A3-B5, and three (87-89) and four (255-258) residues of the N- and C-terminus, respectively, and are indicated by broken lines. Conserved G1-G5 motifs are shown below with consensus sequences and highlighted in yellow. Nonconservative residues that are important for the conformation properties and the catalytic action are found both inside the motifs (highlighted in magenta) and outside the motifs (cyan), respectively.

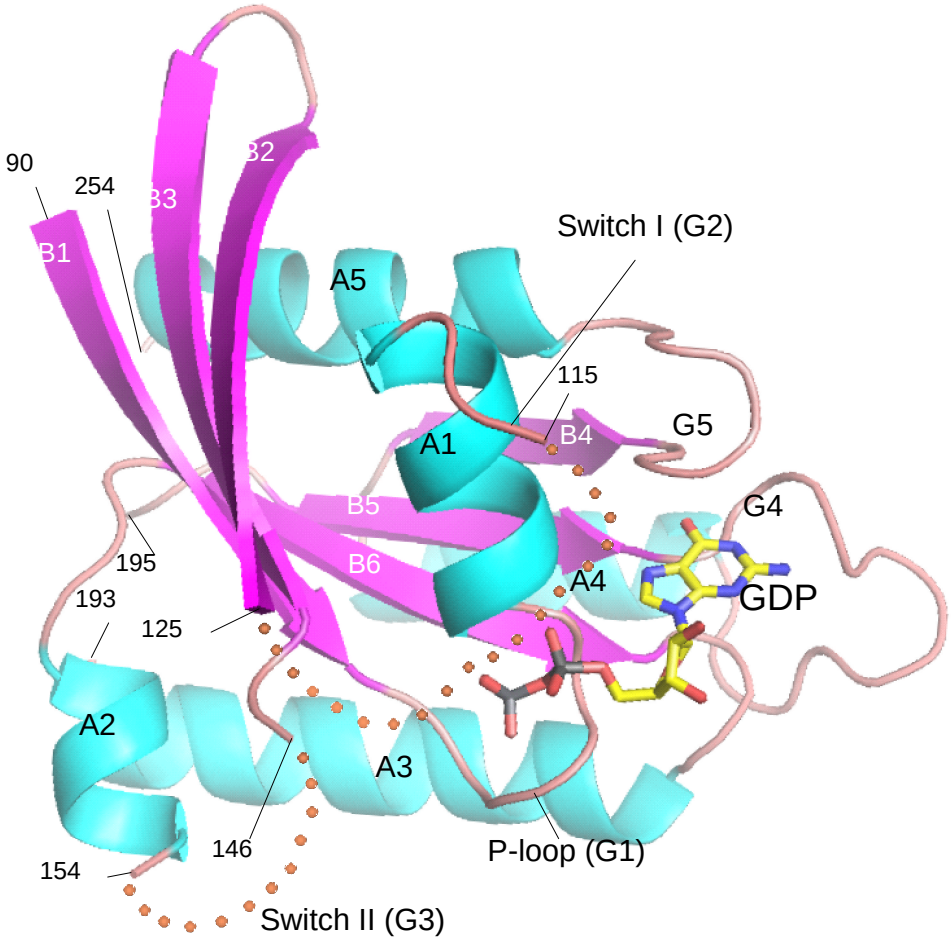

Figure 15. Overall structure of human Rad GTPase

Structure of the Rad GTPase domain bound to GDP. Molecule A is shown with *a*-helices (cyan) and *b*-strands (magenta) with residue numbers.

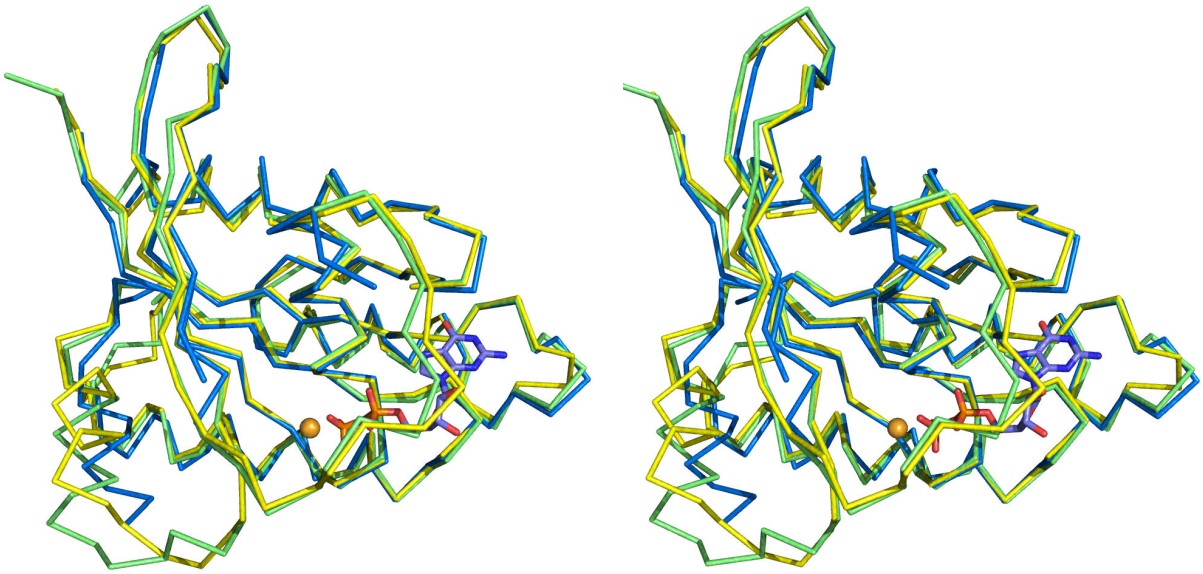

Figure 16. Stereo representation of human Rad GTPase.

Comparison of GTPase domain structures of Rad, H-Ras and RalA bound to GDP. Stereo view of C_α -tracing representation on Rad (blue), H-Ras (yellow), and RalA (green).

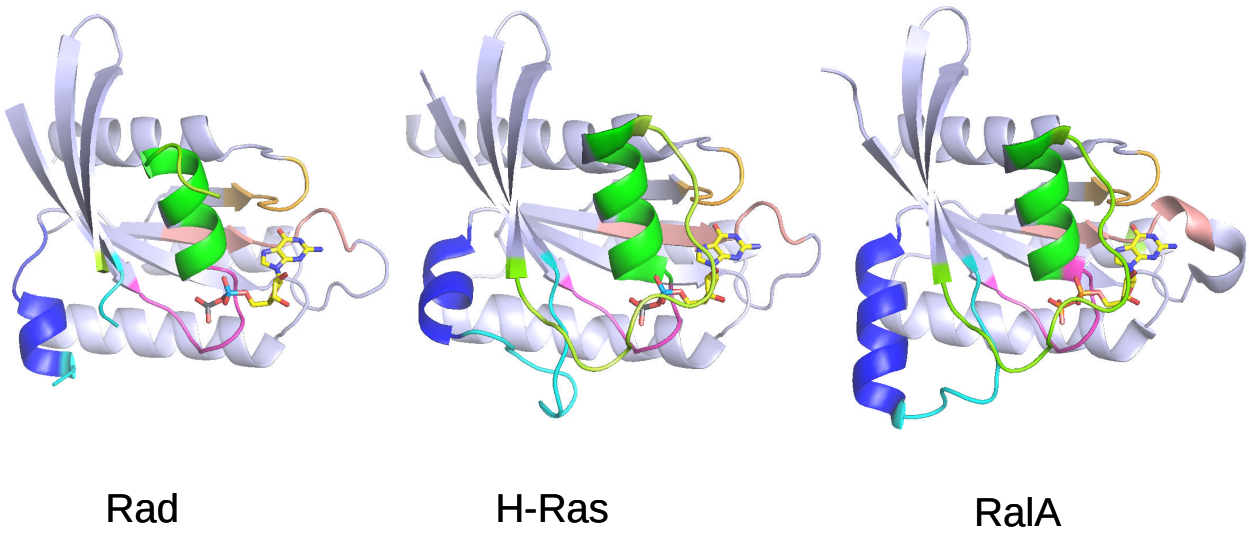

Figure 17. Comparison of length and orientation of switch II of Rad and related small GTPase.

Helix A2 (blue) located in switch II of Rad has different length and orientation compare to the related small GTPases, Ras and RalA.

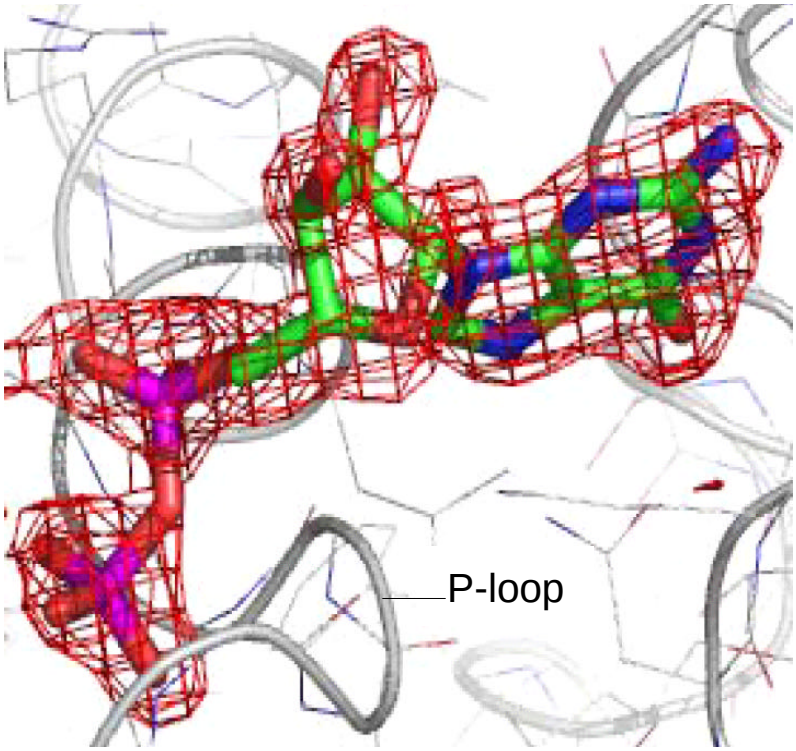

Figure 18. The electron density map of the bound GDP molecule..

The electron density map is drawn at the 2.0 σ level. GDP model is represented as a stick model. The protein is shown as a C_α-tracing tube model with side chain as thin-wire models.

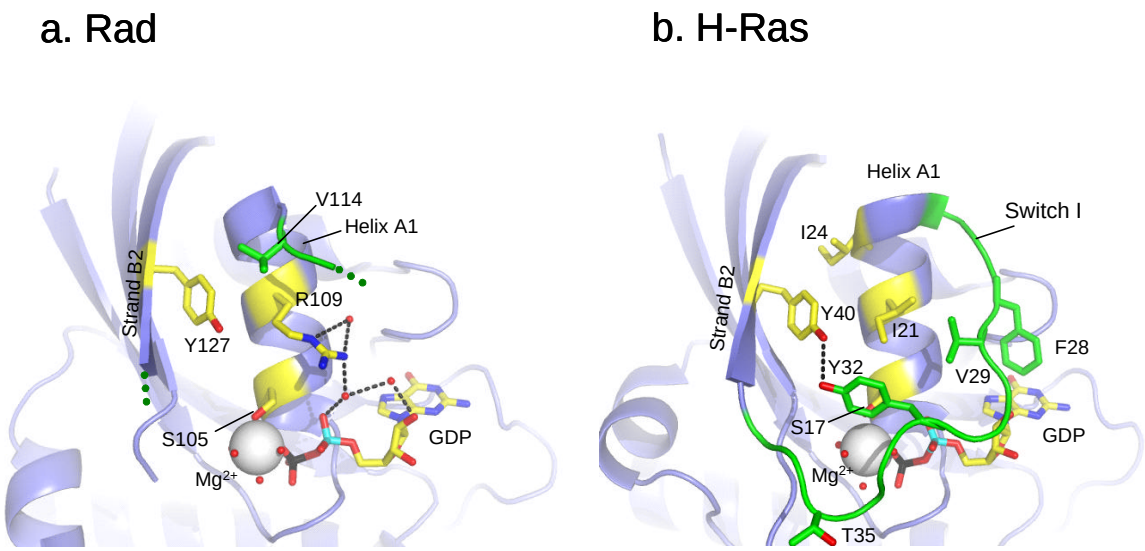

Figure 19. Switch I flexibility

(a) A closeup view of Rad helix A1 and switch I. Most of switch I (green) is disordered. Water molecules are shown as balls (red) and the GDP molecule is represented as stick model with the magnesium ion as a large ball (gray). Hydrogen bonds are indicated by dotted lines.

(b) A closeup view of H-Ras helix A1 and switch I corresponding to (a). H-Ras is the GDP-bound form (1Q21). Switch I (green) covers the GDP molecule with nonpolar interactions between Phe28 and the guanine base. The switch conformation is stabilized by hydrophobic interaction centered by Ile21 and a hydrogen bond between conserved tyrosine residues Tyr32 and Tyr40.

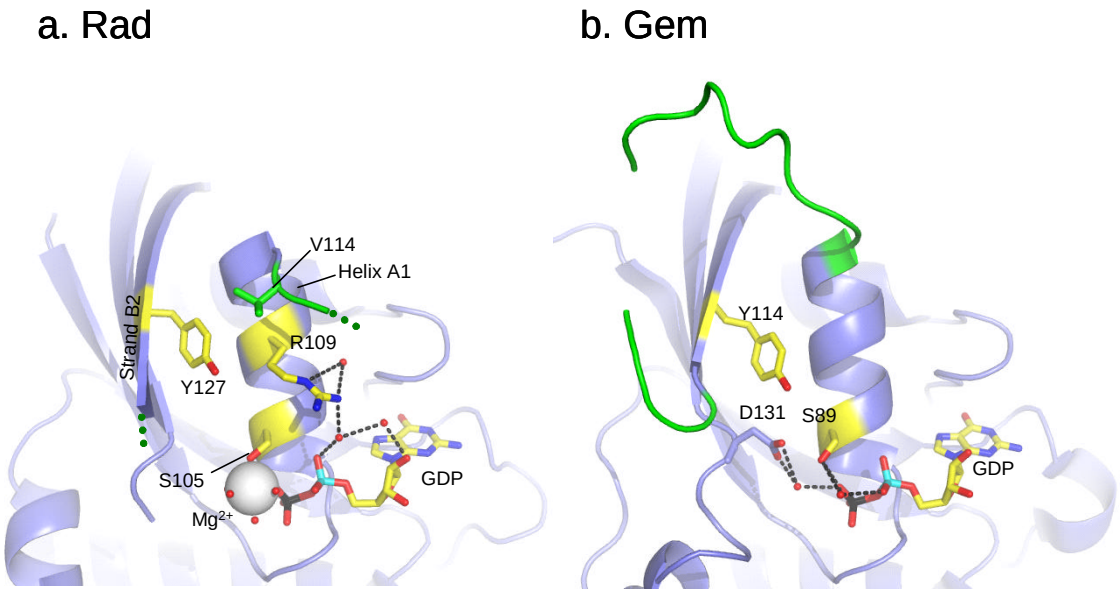

Figure 20. Switch I of the RGK-family members

Both crystal structures of the RGK family members, Rad and Gem, showed disordered switch I regions (green), which would imply the flexibility of the switch parts. No direct contact was observed between the bound GDP molecule and the ordered switch I part in both crystals.

(a) A closeup view of Rad helix A1 and switch I. the same as in Figure 19(a).

(b) A closeup view of Gem helix A1 and switch I corresponding to (a). The crystal contains the GDP-bound form of Gem but no magnesium ion.

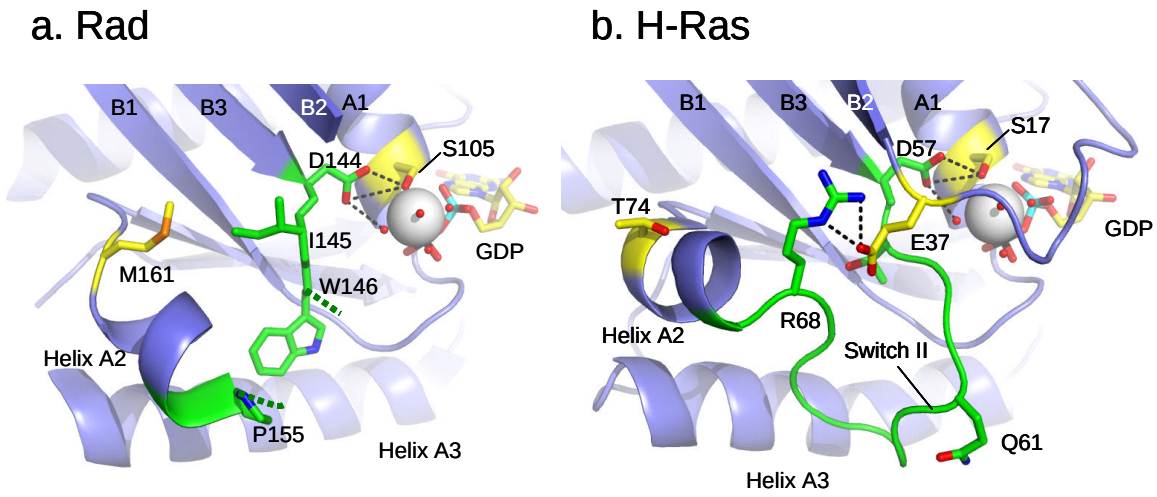

Figure 21. Switch II flexibility

(a) A closeup view of Rad switch II and helix A2. The loop region (147-153) of switch II (green) is disordered. Hydrogen bonds indicated by dotted lines.

(b) A closeup view of H-Ras switch II and helix A2 corresponding to (a).

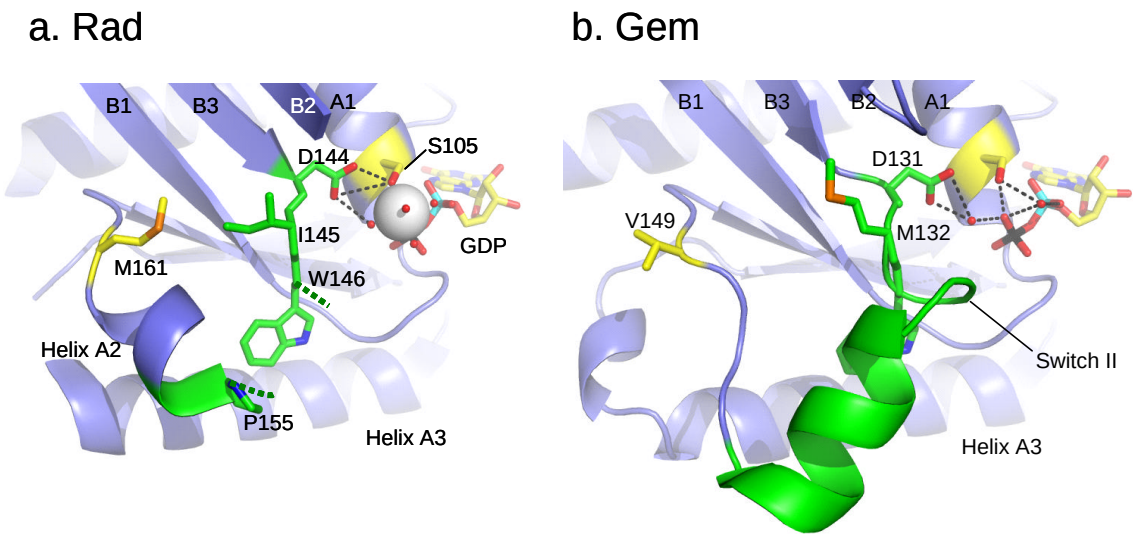

Figure 22. Switch II of the RGK-family members

Switch II regions (green) of the RGK-family members, (a) Rad and (b) Gem, show large conformation differences. Helix A2 of Rad is shorter than Gem due to helix breaker P155, while that of Gem is longer and shifted toward the N-terminal end of switch II.

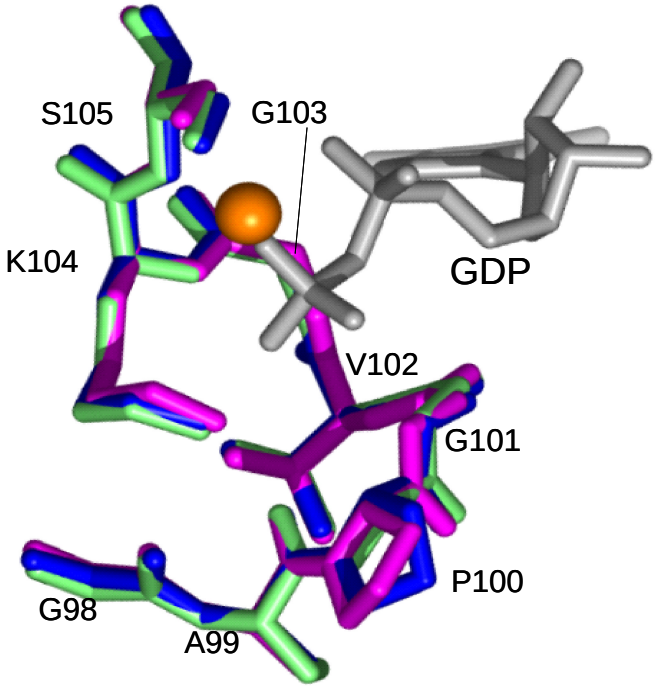

Figure 23. Comparison of the phosphate binding loops of Rad and related small GTPase.

The superimposed segments are GAPGVGKS of Rad (blue) and GAPGVGKS of G12P mutated H-Ras (magenta) and GSGGVGKS of RalA (green). The magnesium ion is represented as a large ball (orange).

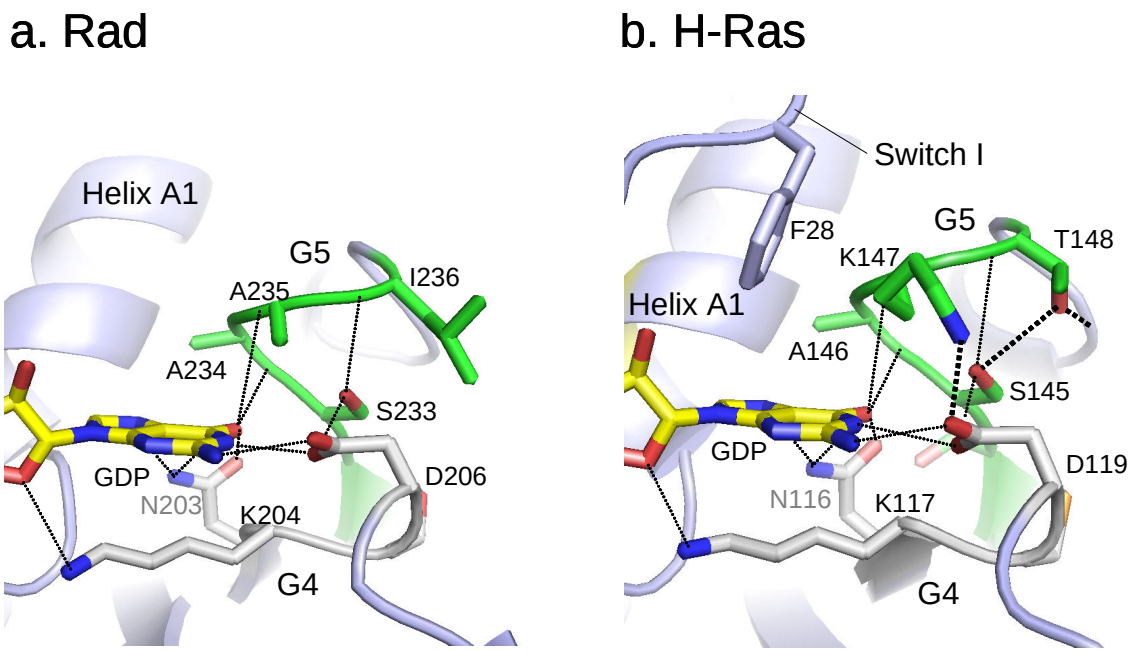

Figure 24. The base recognition loops.

(a) A closeup view of the Rad base-recognition loops. The G4 (LVGNKSDL) and G5 (ETSAAL, green) motifs form loops that interact with the guanine base of GDP. Hydrogen bonds are indicated by thin lines.

(b) A closeup view of the H-Ras base-recognition loops corresponding to (a). The G4 (LVGNKCDL) and G5 (ETSAKT, green) motifs and Phe28 from switch I. Hydrogen bonds indicated by thick lines are absent in the Rad-GDP complex structure shown in (a).

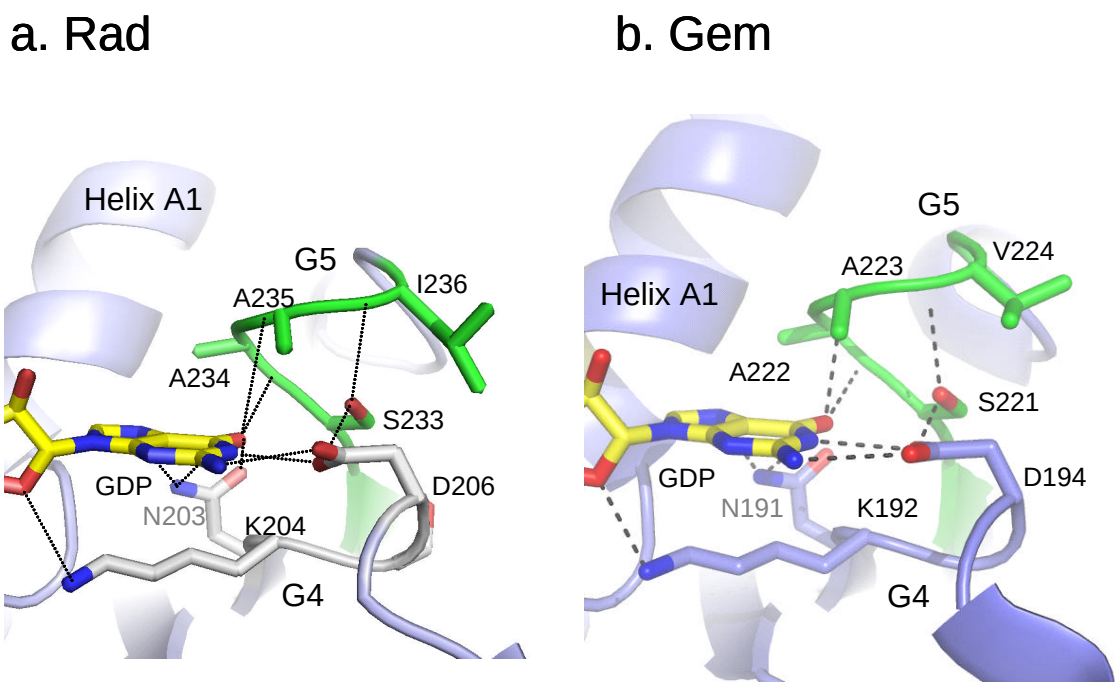

Figure 25. The base recognition loops of RGK-family

The base recognition loops of (a) Rad and (b) Gem show the similar conformation of residues in G4 and G5 that take part in binding to the guanine base.

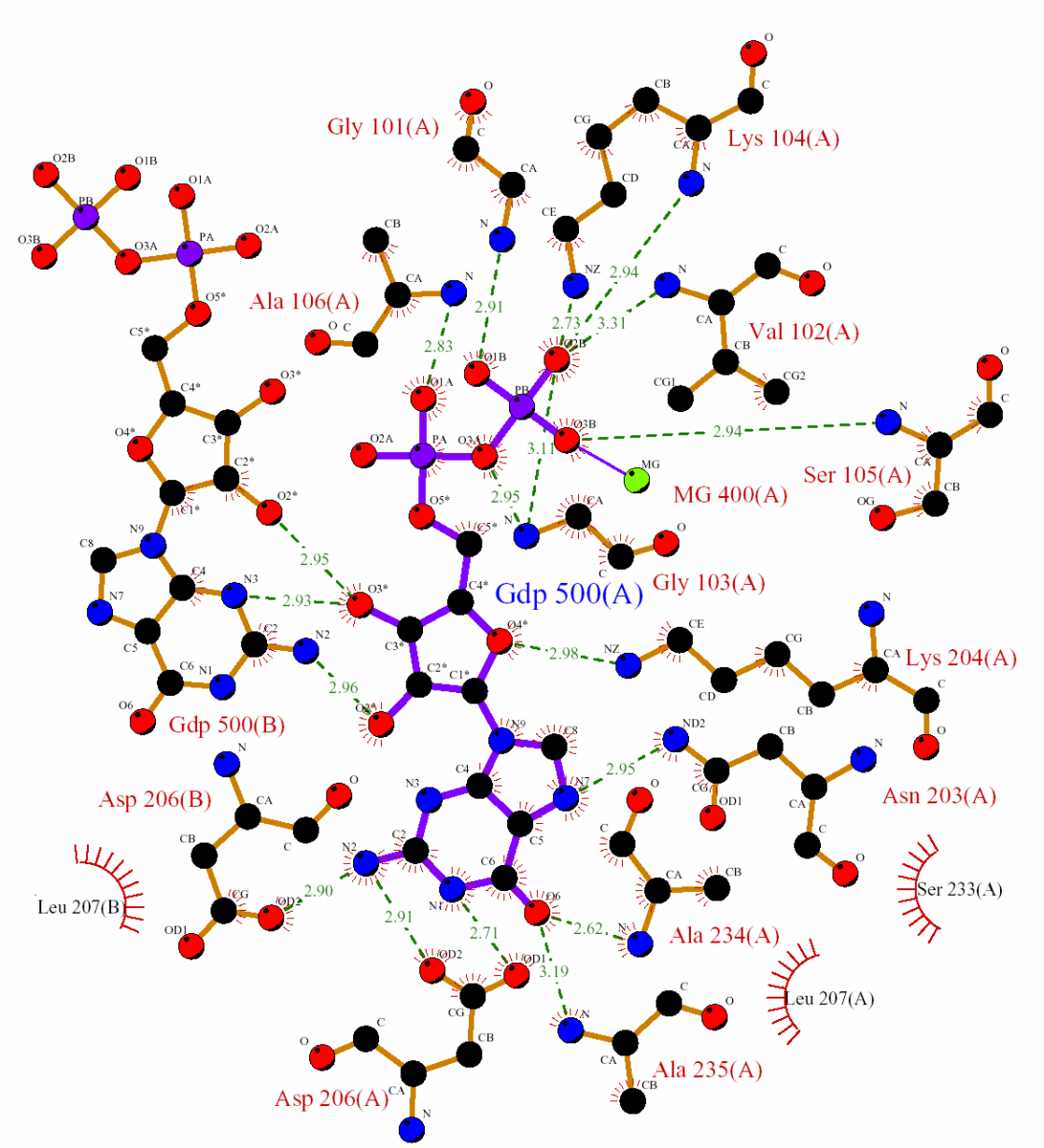

Figure 26. The GDP molecule bound to Rad molecule A

A cartoon shows GDP binding to Rad GTPase molecule A. Hydrogen bonding interactions to Rad residues are indicated by dashlines while hydrophobic contacts are represented by arcs with spokes radiating towards the ligand atoms with which they contact. Three hydrogen bonds are also shown between two GDP molecules bound to the crystallographic independent Rad molecules in the crystals.

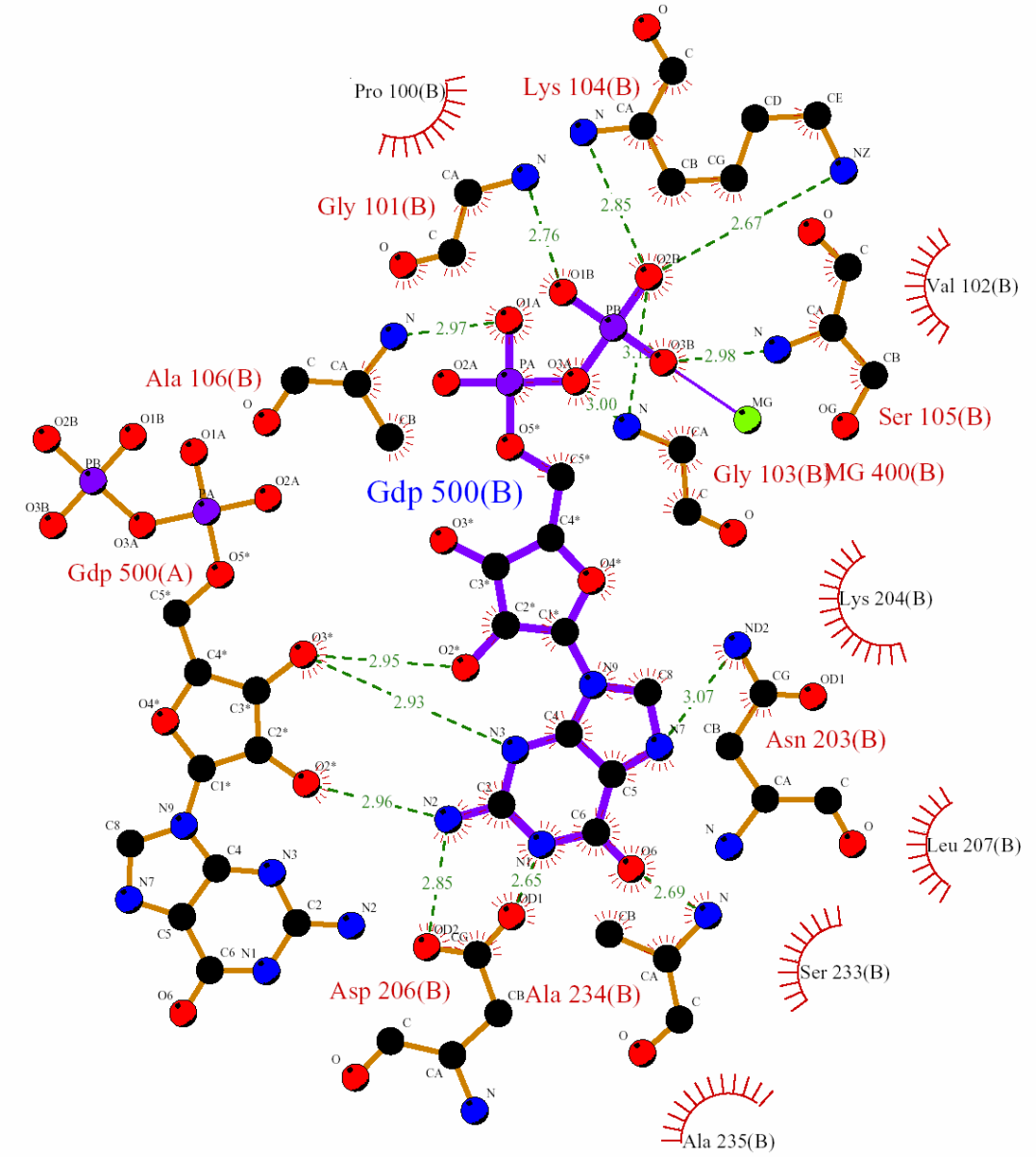

Figure 27. The GDP molecule bound to Rad molecule B

a

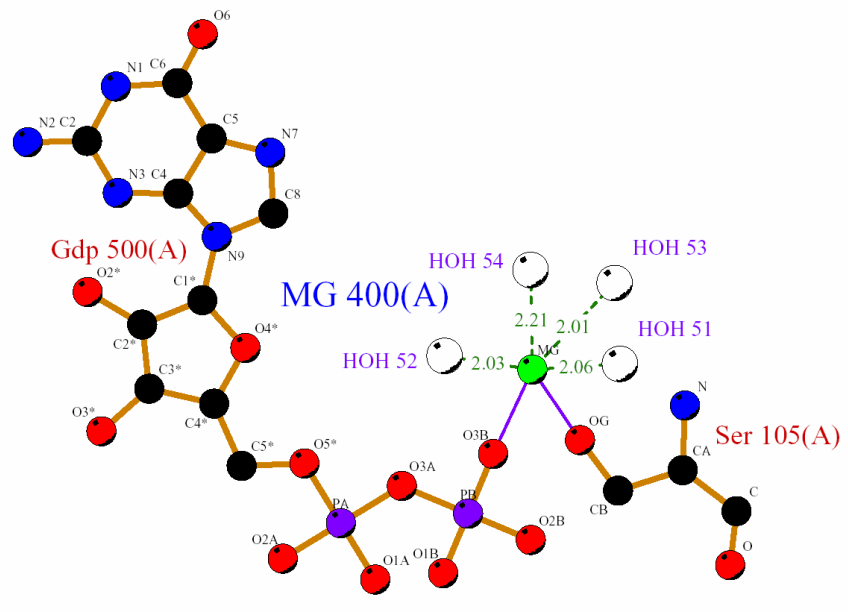

b

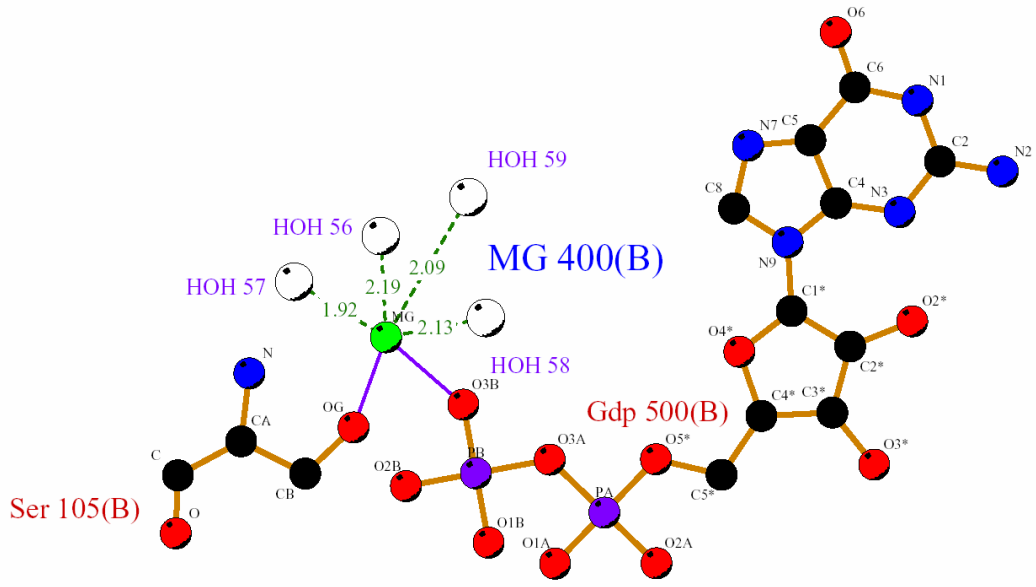

Figure 28. Magnesium ion binding

The magnesium ion from each Rad molecule (a) A and (b) B shows the octahedral coordination shell consisting of four water molecules with indicated number, the oxygen atom of the serine side chain, and the β-phosphate oxygen atom of the GDP molecule.

IV. Discussion

We have for the first time crystallized (Yanuar et al. 2005) and determined the three-dimensional structure of a member of the RGK family GTPases. This Rad structure revealed disordered structures of switches I and II in the GDP-bound form. It shows that the conformational flexibility of both switches is caused by nonconservative substitution in the G2 and G3 motifs together with other substitutions in the structural elements interacting with the switches. Additionally, glycine-rich sequences of the Rad switches would contribute to the flexibility. These observations are distinct from those of H-Ras and most other small GTPases. Compared with H-Ras, there are differences in interactions between switch I and GDP.

Recently, the crystal structure of the GDP-bound form of Gem has been reported. Gem also show the flexibility in the switch I region. Unexpectedly, the switch II loop, that found in Ras, appear as helices with 10 residues in Gem with new orientation and shifted to the N-terminal end of the loop. Nevertheless, the GDP molecule of Rad and Gem adopts a similar conformation to that bound to H-Ras and is located in the same position. This similarity seems to be achieved by the conserved interactions with the guanine base recognition site and the magnesium ion that has typical octahedral coordination shell identical to that in H-Ras. Interestingly, there is no magnesium ion present in the Gem GDP-bound form and also only two water molecules were found near the β-phosphate of GDP or around the magnesium ion position that is usually found in Rad and Ras, suggesting nucleotide binding in Gem is weak.

GTPase-activating proteins (GAPs) generally interact with both switches I and II of target GTPases for their stimulation activity (Vetter and Wittinghofer 2001; Hakoshima et al. 2003). Since the conformational properties of Rad switches I and II are distinct from the Ras-family members including H-Ras, Rad should resists the action of Ras-specific GAPs. Indeed, known GAPs such as Ras-GAP, NF1, p190, Rap-GAP and IQGAP1 failed to stimulate Rad GTPase activity (Zhu et al. 1995). A recently found nm23-H1 was reported to exert a GAP action against Rad as well as a GEF action (Zhu et al. 1999).

The structure of the GDP-bound form of Rad displayed uncommon structural features of the human Rad GTPase domain, especially conformational flexibility in the switch I region. Conformational flexibility is also showed switch I of GDP-bound form of Gem as a member of RGK-family. These findings provide valuable clues for further biochemical and biomedical analyses of this novel small GTPase that might play some important roles in cytoskeletal rearrangement, ion channel regulation, diabetes and cancer.

V. Conclusion

Overexpression, purification and crystallization and preliminary crystallographic studies of GTPase domain of human Rad were performed (Yanuar et al. 2005). The crystals were growth in 2-3 days at 293 K. The crystals were found to belong to space group $P2_1$, with unit-cell parameters a=52.2, b=58.6, c=53.4Å, b=97.9° containing two Rad molecules in the crystallographic asymmetric unit. A diffraction data set was collected to a resolution of 1.8 Å

The crystal structure of human Rad GTPase complex with GDP and Mg^{2+} ion was determined by molecular replacement methods with R_{cryst} 21.42 % and R_{free} 24.01 %. It was found that the overall structure of Rad is similar to those the other small GTPases such as H-Ras and RalA. The GDP molecule is located at the same position as in H-Ras and adopts a similar conformation as that bound in H-Ras.

The structure show conformational flexibility of switches I and II in the GDP-bound form that is caused by (i) nonconservative substitution in the G2 and G3 motifs, (ii) substitutions in the structural elements interacting with the switches and (iii) glycine-rich sequences of the Rad switches.

The structure of the GDP-bound form of Rad showed some unusual structural characteristics of the human Rad GTPase domain that lead to the important pattern for further research in biochemical and biomedical of this novel small GTPase that is closely engaged in cytoskeletal rearrangement, ion channel regulation, diabetes and cancer.

Acknowledgements

BismilLlahirrahmaanirrahiem.
In the name of Allah, the Most Gracious, the Most Merciful.

Firt time, I would like to express my thankful to my parent for their encourage me to reach a high level of education and never stop praying for me.

I would like to express my respect and gratitude to Prof. Toshio Hakoshima for his great supervision, discussion, inspiration and opening during my study in NAIST. My respect and appreciation also should be address to Prof. Akira Isogai for his invaluable helpful for the first time to facilitate and supervise my the study in NAIST.

I also would like to express my special respect and gratitude to my “mother” in Japan, Mrs Sachiko Iida for her invaluable support during this study by an Iida International Student Scholarship from Japan Educational Exchanges and Services.

I would like to thank Drs. K. Kaibuchi and Dr. H. Yamaguchi for providing the human Rad cDNA and for the subcloning, respectively. I also thank to Dr. Ken Kitano and Dr. Shigeru Sakurai for their disscussion and assitance during the study on my topics. Thank you also for all friends in Hakoshima Laboratory for kind and friendly.

Very special thank and love to my wife, Dwi Astuti Cahyasiwi, my children: Nadia Maghfira Ramadhani, Mafaza Hanifa, Muhammad Aqil Fakhri for their love, encourage, prayer and patience. This dissertation is also dedicated and presented to my new children, Hana Fahmida. Thanks also to my brother, sister and big families for their prayer of my success. May God bless all of us. Amien

AlhamduliLlahirrabil’alamien.
All Praise to Allah, the Creator of the universe.

Nara, August 2006
Arry Yanuar

References

Beguin, P., Mahalakshmi, R. N., Nagashima, K., Cher, D. H., Ikeda, H., Yamada, Y., Seino, Y., and Hunziker, W. (2006). Nuclear Sequestration of beta-Subunits by Rad and Rem is Controlled by 14-3-3 and Calmodulin and Reveals a Novel Mechanism for Ca(2+) Channel Regulation. *J Mol Biol*, **355**(1), 34-46.

Beguin, P., Nagashima, K., Gonoi, T., Shibasaki, T., Takahashi, K., Kashima, Y., Ozaki, N., Geering, K., Iwanaga, T., and Seino, S. (2001). Regulation of Ca2+ channel expression at the cell surface by the small G-protein kir/Gem. *Nature*, **411**(6838), 701-6.

Berman, H. M., Westbrook, J., Feng, Z., Gilliland, G., Bhat, T. N., Weissig, H., Shindyalov, I. N., and Bourne, P. E. (2000). The Protein Data Bank. *Nucl. Acids Res.*, **28**(1), 235-242.

Brünger, A. T., Adams, P. D., Clore, G. M., DeLano, W. L., Gros, P., Grosse-Kunstleve, R. W., Jiang, J.-S., Kuszewski, J., Nilges, M., Pannu, N. S., Read, R. J., Rice, L. M., Simonson, T., and Warren, G. L. (1998). Crystallography & NMR System: A New Software Suite for Macromolecular Structure Determination. *Acta Crystallogr D. Biol. Crystallogr.*, **54**, 905-921.

CCP4 (Collaborative Computational Project), N. (1994). The CCP4 suite: programs for protein crystallography. *Acta Crystallogr D. Biol. Crystallogr.*, **D50**(5), 757-759.

Claude, J. B., Suhre, K., Notredame, C., Claverie, J. M., and Abergel, C. (2004). CaspR: a web server for automated molecular replacement using homology modelling. *Nucleic Acids Res*, **32**(Web Server issue), W606-9.

Cohen, L., Mohr, R., Chen, Y. Y., Huang, M., Kato, R., Dorin, D., Tamanoi, F., Goga, A., Afar, D., Rosenberg, N., and et al. (1994). Transcriptional activation of a ras-like gene (kir) by oncogenic tyrosine kinases. *Proc Natl Acad Sci U S A*, **91**(26), 12448-52.

Crowther, R. A. (1972). *The Molecular Replacement Method*. in "Int. Sci. Rev. No 13," Rossmann, M. G., ed. (New York: Gordon and Breach), pp. 173-178.

Crowther, R. A., and Blow, D. M. (1967). A method of positioning a known molecule in an unknown crystal structure. *Acta Crystallogr*, **23**, 544-548.

DeLano, W. L., and Bromberg, S. (2004). Pymol. User Guide (http://www.pymol.org). San Carlos, California, DeLano Scientific, LLC.

Doria, A., Caldwell, J. S., Ji, L., Reynet, C., Rich, S. S., Weremowicz, S., Morton, C. C., Warram, J. H., Kahn, C. R., and Krolewski, A. S. (1995). Trinucleotide repeats at the rad locus. Allele distributions in NIDDM and mapping to a 3-cM region on chromosome 16q. *Diabetes*, **44**(2), 243-7.

Finlin, B. S., Crump, S. M., Satin, J., and Andres, D. A. (2003). Regulation of voltage-gated calcium channel activity by the Rem and Rad GTPases. *Proc Natl Acad Sci U S A*, **100**(24), 14469-74.

Hakoshima, T., Shimizu, T., and Maesaki, R. (2003). Structural basis of the Rho GTPase signaling. *J Biochem (Tokyo)*, **134**(3), 327-31.

Herrmann, C. (2003). Ras-effector interactions: after one decade. *Current Opinion in Structural Biology*, **13**(1), 122-129.

Ihara, K., Muraguchi, S., Kato, M., Shimizu, T., Shirakawa, M., Kuroda, S., Kaibuchi, K., and Hakoshima, T. (1998). Crystal structure of human RhoA in a dominantly active form complexed with a GTP analogue. *J Biol Chem*, **273**(16), 9656-66.

Jones, T. A., and Kjeldgaard, M. (1997). *[10] Electron-density map interpretation, Methods in Enzymology*. in "Macromolecular Crystallography Part B," Sweet, C. W. C. J. a. R. M., ed.: Academic Press), 173-208.

Kelly, K. (2005). The RGK family: a regulatory tail of small GTP-binding proteins. *Trends Cell Biol*, **15**(12), 640-3.

Krengel, U., Schlichting, L., Scherer, A., Schumann, R., Frech, M., John, J., Kabsch, W., Pai, E. F., and Wittinghofer, A. (1990). Three-dimensional structures of H-ras p21 mutants: molecular basis for their inability to function as signal switch molecules. *Cell*, **62**(3), 539-48.

Laskowski, R. A., MacArthur, M. W., Moss, D. S., and Thornton, J. M. (1993). PROCHECK: a program to check the stereochemical quality of protein structures. *J. Appl. Crystallogr.*, **26**, 283-291.

Maguire, J., Santoro, T., Jensen, P., Siebenlist, U., Yewdell, J., and Kelly, K. (1994). Gem: an induced, immediate early protein belonging to the Ras family. *Science*, **265**(5169), 241-4.

Matthews, B. W. (1968). Solvent content of protein crystals. *J Mol Biol*, **33**(2), 491-7.

Moyers, J. S., Bilan, P. J., Reynet, C., and Kahn, C. R. (1996). Overexpression of Rad inhibits glucose uptake in cultured muscle and fat cells. *J Biol Chem*, **271**(38), 23111-6.

Moyers, J. S., Bilan, P. J., Zhu, J., and Kahn, C. R. (1997). Rad and Rad-related GTPases interact with calmodulin and calmodulin-dependent protein kinase II. *J Biol Chem*, **272**(18), 11832-9.

Nicely, N. I., Kosak, J., de Serrano, V., and Mattos, C. (2004). Crystal structures of Ral-GppNHp and Ral-GDP reveal two binding sites that are also present in Ras and Rap. *Structure*, **12**(11), 2025-36.

Olson, M. F. (2002). Gem GTPase: between a ROCK and a hard place. *Curr Biol*, **12**(14), R496-8.

Otwinowski, Z., and Minor, W. (1997). [20] Processing of X-ray diffraction data collected in oscillation mode. *Methods in Enzymology*, **276**, 307-326.

Pai, E. F., Krengel, U., Petsko, G. A., Goody, R. S., Kabsch, W., and Wittinghofer, A. (1990). Refined crystal structure of the triphosphate conformation of H-ras p21 at 1.35 A resolution: implications for the mechanism of GTP hydrolysis. *Embo J*, **9**(8), 2351-9.

Read, R. J. (1986). Improved Fourier coefficients for maps using phases from partial structures with errors. *Acta Crystallogr A. Foundation of Crystallogr.*, **42**, 140-149.

Reynet, C., and Kahn, C. R. (1993). Rad: a member of the Ras family overexpressed in muscle of type II diabetic humans. *Science*, **262**(5138), 1441-4.

Rossmann, M. G., and Blow, D. M. (1962). The detection of sub-units within the crystallographic asymmetric unit. *Acta Crystallogr*, **15**, 24-31.

Sali, A., and Blundell, T. L. (1993). Comparative Protein Modelling by Satisfaction of Spatial Restraints. *Journal of Molecular Biology*, **234**(3), 779-815.

Takai, Y., Sasaki, T., and Matozaki, T. (2001). Small GTP-binding proteins. *Physiol Rev*, **81**(1), 153-208.

Terwilliger, T. C. (2003). SOLVE and RESOLVE: Automated Structure Solution and Density Modification. *Methods in Enzymology*, **374**, 22-37.

Thompson, G., Owen, D., Chalk, P. A., and Lowe, P. N. (1998). Delineation of the Cdc42/Rac-binding domain of p21-activated kinase. *Biochemistry*, **37**(21), 7885-91.

Tong, L. A., de Vos, A. M., Milburn, M. V., and Kim, S. H. (1991). Crystal structures at 2.2 A resolution of the catalytic domains of normal ras protein and an oncogenic mutant complexed with GDP. *J Mol Biol*, **217**(3), 503-16.

Tseng, Y. H., Vicent, D., Zhu, J., Niu, Y., Adeyinka, A., Moyers, J. S., Watson, P. H., and Kahn, C. R. (2001). Regulation of growth and tumorigenicity of breast cancer cells by the low molecular weight GTPase Rad and nm23. *Cancer Res*, **61**(5), 2071-9.

Vagin, A., and Teplyakov, A. (1997). MOLREP: an Automated Program for Molecular Replacement. *Journal of Applied Crystallography*, **30**(6), 1022-1025.

Vetter, I. R., and Wittinghofer, A. (2001). The guanine nucleotide-binding switch in three dimensions. *Science*, **294**(5545), 1299-304.

Ward, Y., Yap, S. F., Ravichandran, V., Matsumura, F., Ito, M., Spinelli, B., and Kelly, K. (2002). The GTP binding proteins Gem and Rad are negative regulators of the Rho-Rho kinase pathway. *J Cell Biol*, **157**(2), 291-302.

Yanuar, A., Sakurai, S., Kitano, K., and Hakoshima, T. (2005). Expression, purification, crystallization and preliminary crystallographic analysis of human Rad GTPase. *Acta Crystalogr F Struct. Biol. Cryst. Commun*, **F61**(11), 978-980.

Zhu, J., Reynet, C., Caldwell, J. S., and Kahn, C. R. (1995). Characterization of Rad, a new member of Ras/GTPase superfamily, and its regulation by a unique GTPase-activating protein (GAP)-like activity. *J Biol Chem*, **270**(9), 4805-12.

Zhu, J., Tseng, Y. H., Kantor, J. D., Rhodes, C. J., Zetter, B. R., Moyers, J. S., and Kahn, C. R. (1999). Interaction of the Ras-related protein associated with diabetes rad and the putative tumor metastasis suppressor NM23 provides a novel mechanism of GTPase regulation. *Proc Natl Acad Sci U S A*, **96**(26), 14911-8.